LA-4237-MS

LOS ALAMOS SCIENTIFIC LABORATORY
of the
University of California
LOS ALAMOS • NEW MEXICO

CMF-13 Research on Carbon and Graphite

Report No. 10

Summary of Progress from May 1 to July 31, 1969

UNITED STATES
ATOMIC ENERGY COMMISSION
CONTRACT W-7405-ENG. 36

This LA. . .MS report presents the summary of progress of CMF-13 research on carbon and graphite at LASL. Previous summary of progress reports in this series, all unclassified, are:

LA-3693-MS
LA-3758-MS
LA-3821-MS
LA-3872-MS
LA-3932-MS
LA-3989-MS
LA-4057-MS
LA-4128-MS
LA-4171-MS

This report, like other special-purpose documents in the LA. . .MS series, has not been reviewed or verified for accuracy in the interest of prompt distribution.

Distributed: September 3, 1969

LA-4237-MS
SPECIAL DISTRIBUTION

LOS ALAMOS SCIENTIFIC LABORATORY
of the
University of California
LOS ALAMOS • NEW MEXICO

CMF-13 Research on Carbon and Graphite

Report No. 10

Summary of Progress from May 1 to July 31, 1969*

by

Morton C. Smith

*Supported in part by the Office of Advanced Research and Technology of the National Aeronautics and Space Administration.

CMF-13 RESEARCH ON CARBON AND GRAPHITE

REPORT NO. 10: SUMMARY OF PROGRESS FROM MAY 1 TO JULY 31, 1969

I. INTRODUCTION

This is the tenth in a series of progress reports devoted to carbon and graphite research in LASL Group CMF-13, and summarizes work done during the months of May, June and July, 1969. It should be understood that in such a progress report many of the data are preliminary, incomplete, and subject to correction, and many of the opinions and conclusions are tentative and subject to change. This report is intended only to provide up-to-date background information to those who are interested in the materials and programs described in it, and should not be quoted or used as a reference publicly or in print.

Research and development on carbon and graphite were undertaken by CMF-13 primarily to increase understanding of their properties and behavior as engineering materials, to improve the raw materials and processes used in their manufacture, and to learn how to produce them with consistent, predictable, useful combinations of properties. The approach taken is microstructural, based on study and characterization of natural, commercial, and experimental carbons and graphites by such techniques as x-ray diffraction, electron and optical microscopy, and porosimetry. Physical and mechanical properties are measured as functions of formulation, treatment, and environmental variables, and correlations are sought among properties and structures. Raw materials and manufacturing techniques are investigated, improved, and varied systematically in an effort to create specific internal structures believed to be responsible for desirable combinations of properties. Prompt feedback of information among these activities then makes possible progress in all of them toward their common goal of understanding and improving manufactured carbons and graphites.

Since its beginning, this research has been sponsored by the Division of Space Nuclear Systems of the United States Atomic Energy Commission, through the Space Nuclear Propulsion Office. More recently additional general support for it has been provided by the Office of Advanced Research and Technology of the National Aeronautics and Space Administration. Many of its facilities and services have been furnished by the Division of Military Applications of AEC. The direct and indirect support and the guidance and encouragement of these agencies of the United States Government are gratefully acknowledged.

II. SANTA MARIA COKE

A. General

The initial CMF-13 investigations of the internal structure, properties, behavior and potential usefulness of Santa Maria coke as a filler material for graphite manufacture were summarized in the last previous report in this series, LA-4171-MS. Since that report was written, the further investigations of this very unusual raw material have been concerned principally with its microstructure and its grinding, packing and extrusion behavior.

B. Internal Structure (R. D. Reiswig, L. S. Levinson, J. A. O'Rourke)

As was described in LA-4171-MS, a structural feature which is very common in Santa Maria coke, but otherwise extremely rare, is a spheroidal unit, commonly 30 μ or less in diameter, within which lamellae composed of layers of carbon atoms appear to have grown radially from a common center. At least after the coke has been calcined or graphitized, a fracture through such a spheroid tends to follow weak zones between the radiating lamellae, and

Fig. 1. Rosette patterns on the fracture surface of a lump of Santa Maria coke which had been graphitized at 2700°C. 5000 X.

Fig. 2. Irregular structure between rosettes on the same fracture surface shown in Fig. 1. 5000 X.

so to pass through or near its center. The result is a striking rosette pattern on the fracture surface, of the type shown in Fig. 1. Since these spheroids do not constitute the entire volume of the coke, there are also many regions on the fracture surface within which the structure is quite irregular. Such a region is shown in Fig. 2. Even where rosettes are not visible, it appears in some areas that the principal structural units are warped platelets, not unlike single petals or groups of petals from the rosettes of Fig. 1. More generally, however, the matrix structure seems to be finer and less well organized than is the petal structure of the rosettes.

Optical and electron micrographs of many rosettes appearing on fracture surfaces and on polished sections have been examined for evidence of a nucleating agent which might have initiated radial growth from the center of the rosette. None has been found. The centers of the rosettes often appear to be more dense than the material around them. This, however, may result simply from symmetrical shrinkage during coking of spheroids formed, for example, by separation of a mesophase. On the other hand it may indicate that the nucleating agent was an organic species which, upon pyrolysis, left an unusually dense carbon residue.

Electron-beam microprobe scans have been made on Santa Maria coke in the green,calcined, and graphitized conditions. On a section through the green coke the electron beam produced a crater and left a microscopically visible trace in regions between rosettes, but had no visible effect on material composing the rosettes themselves. Apparently the volatile content of the coke is low within the rosettes, and relatively high elsewhere. Only vanadium and sulfur were detected spectrographically during these scans, and both elements appeared to be distributed quite uniformly throughout the green coke. (The characteristic radiation of vanadium was actually slightly more intense from material composing rosettes than from the more volatile matrix around them. This, however, is believed to have resulted from differences in density and organic chemical composition rather than from real differences in vanadium concentration.)

Microprobe scans of the calcined coke indicated that

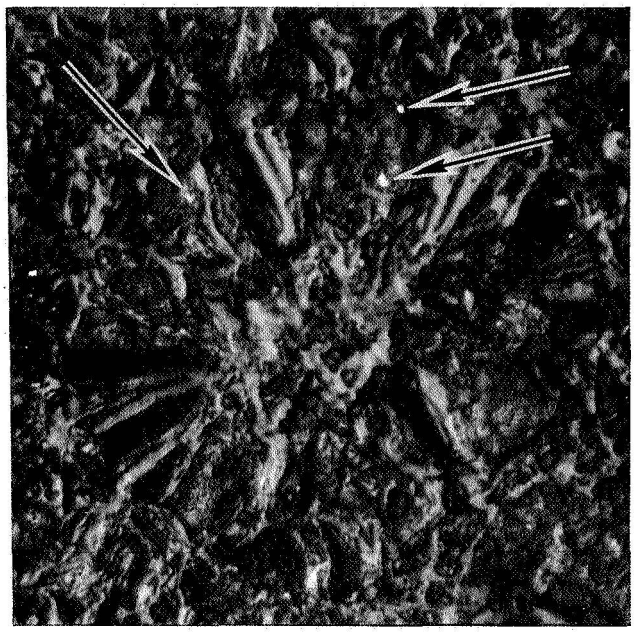

Fig. 3. Metallic-appearing inclusions, believed to be vanadium carbide, in Santa Maria coke graphitized at 2800°C. 2000 X, hydrogen-ion etch.

the more volatile material had been effectively removed by the calcining operation. The electron beam produced no visible cratering either within or outside of the rosettes, and both vanadium and sulfur were still quite uniformly distributed.

Sections through lumps of Santa Maria coke which had been graphitized for 1/2 hr at 2800°C were observed microscopically to contain very small metallic-appearing inclusions such as those indicated in Fig. 3. In a few cases these occurred in concentrated groups near particle surfaces. In general, however, the inclusions were randomly distributed throughout the coke lumps, in no obvious relation to their rosette or matrix structures. The microprobe revealed that all of these inclusions were very high in vanadium content, and they are believed to be vanadium carbide. No vanadium or other impurity element was detected elsewhere in the coke structure. The randomness of distribution of these particles in the graphitized material and the uniform distribution of vanadium in the green and calcined cokes make it appear unlikely that vanadium is involved in nucleation of the spheroidal structures observed in Santa Maria coke.

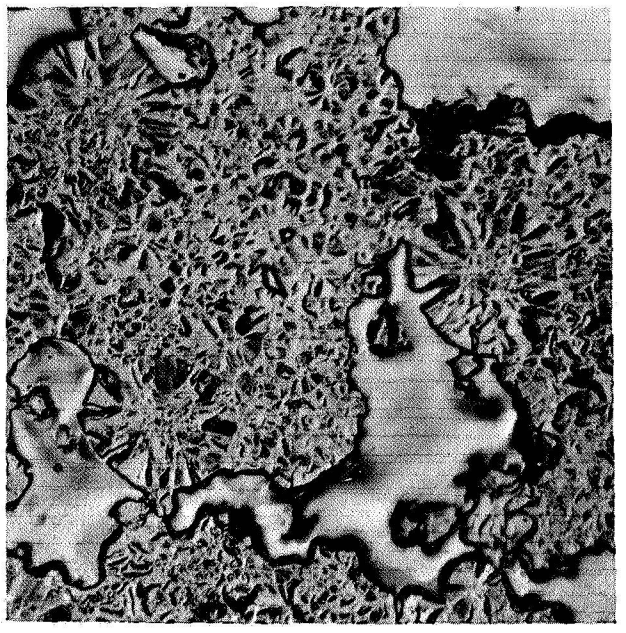

Fig. 4. Spheroids in Santa Maria coke projecting into gas bubbles in the coke lump. Light gray areas are voids filled with epoxy mounting resin. 500 X, hydrogen-ion etch.

Optical and electron microscopy and microprobe analysis all show that these spheroids tend to appear in groups or clusters, with the less regularly structured matrix between or around them. As is illustrated by Fig. 4, the spheroids occasionally intrude into gas bubbles in the coke structure, and in general they are fully developed and quite symmetrical where they do so. Quite probably they form early in the coking process, and are surrounded by liquid as they form and grow to essentially their final sizes. The liquid around them then is expelled locally by the expanding gases which form the bubbles. From the relatively low volatile content of material composing the spheroids it appears that they may form by polymerization of a specific organic component of the charge to the coker. In doing so they would reject other organic species into the remaining fluid around them, which would subsequently form the matrix structure. Although the spheroids tend to form in colonies, they are present in every coke lump that has so far been examined. The nucleating agent, then -- if there was one -- was disseminated throughout the contents of the coker. In the absence of concentrations of inorganic elements, such an agent would apparently have been organic in nature. No real uniformity is obvious in the internal structures of the spheroids, but sections through them commonly appear to have six to eight petals per rosette -- suggesting some regularity in internal structure, and perhaps a steric effect of a nucleating agent. In fact, however, a history of nucleation and growth has not so far been established for the spheroids, and speculation concerning their formation should not at this point ignore such other possibilities as separation of a peculiarly structured mesophase early in the coking process.

C. Grinding (R. J. Imprescia, H. D. Lewis)

A series of laboratory-scale grinding experiments on Santa Maria coke, largely in the green or the calcined condition, was described in LA-4171-MS. This has been continued using as the grinding feed a lot of Santa Maria LV coke (calcined by the vendor) which had been graphitized at 2700°C by LASL Group CMB-6. The conditions of individual grinding operations are summarized in Table I, which supplements Table IV of LA-4171-MS. Grinding schedules, screen analyses, and filler-particle packing densities (discussed below) for these grinding experiments are listed in Table II. Here the sequence of grinding passes is indicated in column 2, where each letter indicates one pass under the conditions listed opposite that letter in Table I.

One object of these experiments was, if possible, to produce a particle-size distribution similar to that of CMF-13 Lot G-13, a sample of Great Lakes Grade 1008-S graphite flour which has been used successfully at LASL for a variety of purposes. The screen analysis of this reference material is shown at the bottom of Table II. As was reported in LA-4171-MS, a reasonable approximation of this analysis was produced by three stages of hammer milling the lump, calcined, Santa Maria coke. This has proved to be much more difficult when the lump coke was graphitized before grinding.

In the grinding experiments of Series I (Table II) the graphitized lump material was reduced by one pass (F) or two passes (F + H) through hammer mills followed by

TABLE I

GRINDING MILLS, CONDITIONS AND PROCEDURES

Grinding Procedure	Type of Mill	Discharge	Pressure, psi Pusher/Opposite	Feed Rate, g/min[d]
F	Williams hammer mill[a]	Screen, 0.0313-in. dia holes	---	38
G	Weber hammer mill[b]	Screen, 0.008-in. wide slots	---	28
H	Weber hammer mill	Screen, 0.024-in. dia holes	---	28
I	Trost fluid-energy mill[c]	Orifice, 1.25-in. dia	100/100	15
M	Trost fluid-energy mill	Orifice, 1.25-in. dia	100/60	15
O	Trost fluid-energy mill	Orifice, 1.25-in. dia	100/100	7.5
P	Williams hammer mill	Screen, 0.0625-in. dia holes	---	38
Q	Weber hammer mill	Screen, 0.012-in. wide slots	---	28
R	Trost fluid-energy mill	Orifice, 1.25-in. dia	100/50	15
S	Williams hammer mill	Screen, 0.125-in. dia holes	---	90
T	Weber hammer mill	Screen, 0.040-in. dia holes	---	30
U	Trost fluid-energy mill	Orifice, 1.25-in. dia	100/80	28

(a) "Lab" Hammer Mill, Williams Patent Crusher and Pulverizer Co.

(b) Model S500 Laboratory Pulverizing Mill, Weber Bros. and White Metal Works, Inc.

(c) Trost Model GEMTX Laboratory Mill, Trost Jet Mill Division, George W. Helme Co., Inc.

(d) Accurate to about ±5 %.

fluid-energy grinding (I or O). None of the grinding products resembled Lot G-13 in screen analysis. In particular, all contained far too much +80 mesh material.

Comparison of the products of the F and F+H hammer-millings of Series I indicated that the second hammer-milling considerably reduced the proportion of -45+80 mesh material. Therefore in Series II the graphitized lump feed was ground in six successive hammer-millings followed by fluid-energy milling. Indeed the proportion of -45+80 mesh material was progressively reduced by hammer-milling, but instead of being distributed uniformly through the finer screen fractions most of it was simply shifted into the -80+170 mesh fraction. An attempt to reduce this by fluid-energy grinding was successful, but the fluid-energy mill also reduced -- instead of increasing -- the proportion of -170+325 mesh material and yielded an undesirably large proportion of -325 mesh fines.

In grinding some materials it has been observed that a decrease in the number of intermediate steps in the grinding schedule has reduced the proportion of fines produced. In Series III, therefore, only the first (P) and last (G) hammer-millings of Series II were used, followed by fluid-energy milling (I). This shortened procedure had little effect on the screen analyses of the products. After fluid-energy grinding, the final product was identified as Lot GP-12 and was used in extrusion experiments described below.

As was reported in LA-4171-MS, for calcined Santa Maria coke, a decrease in air pressure on the opposing jet of the Trost fluid-energy mill may reduce the proportion of fines produced by it. Therefore in Series IV the same sequence of grinding passes was used as in Series III except that in the final fluid-energy grind the pressure on the opposing jet was reduced to 60 psi from the 100 psi normally used. An unexpected variation in the product of the second hammer-milling (G) invalidated the expected comparison between the products of the two series, so that the effect of this change in mill conditions is not clear. It appears not to have been large, and the final Series IV

TABLE II

GRINDING EXPERIMENTS, GRAPHITIZED SANTA MARIA COKE

Series	Grinding Schedule[a]	Weight Percent in Screen Fraction (U.S. Std. Sieves)						Filler-Particle Packing Density, g/cm^3 [b]	
		+25	-25+45	-45+80	-80+170	-170+325	-325	Stearic Acid	Hot Molding
I	F	0	10	35	35	10	10	1.22	1.44
	F+H	0	10	25	35	10	20	1.27	1.56
	F+H+I	0	trace	30	15	20	35	1.35	1.55
	F+I	0	5	30	15	20	30	1.42	1.55
	F+O	0	5	25	15	10	45	---	1.55
II	P	0	25	30	20	10	15		
	P+H	0	5	25	35	10	25		
	P+2H	0	trace	20	40	10	30		
	P+3H	0	trace	15	42	13	30		
	P+3H+Q	0	trace	10	40	15	35		
	P+3H+Q+G	0	0	6	43	16	36		
	P+3H+Q+G+I	0	trace	5	25	10	60	1.43	1.57
III	P	0	20	35	25	10	10		
	P+G	0	trace	15	30	15	40		
(GP-12)	P+G+I	0	trace	10	25	10	55		
IV	P	5	21	31	23	10	10		
	P+G	0	1.5	22.0	32.5	19.0	25.0		
	P+G+M	0	0.5	19.5	25.0	10.0	45.0	1.50	1.56
V	P	0.5	23.0	35.0	20.0	6.5	15.0		
	P+I	trace	16.0	17.5	17.5	13.5	35.0	1.37	1.56
	P+I+R	0	15.0	18.5	16.5	10.0	40.0		
VI	S	40.0	28.5	14.0	19.5	3.5	4.5		
	S+T	trace	13.5	36.5	28.0	12.5	9.5		
	S+T+U	trace	10.0	32.0	22.0	10.0	26.0	1.59	1.55
GP-14	S+T+U	trace	9.0	31.5	22.0	8.0	29.5		
GP-14	-62# Fraction	0	trace	25.5	29.5	10.0	35.0		
GP-15	S+T+I	0	trace	17.0	27.0	9.0	47.0		
G-13	As-received	0	trace	1.7	26.3	32.6	39.4		

(a) Letters refer to grinding procedures listed in Table I. "2H" and "3H" indicate 2 and 3 consecutive grindings using procedure "H".

(b) The stearic-acid and hot-molding techniques used to measure density of the packed filler particles have been described in LA-3901.

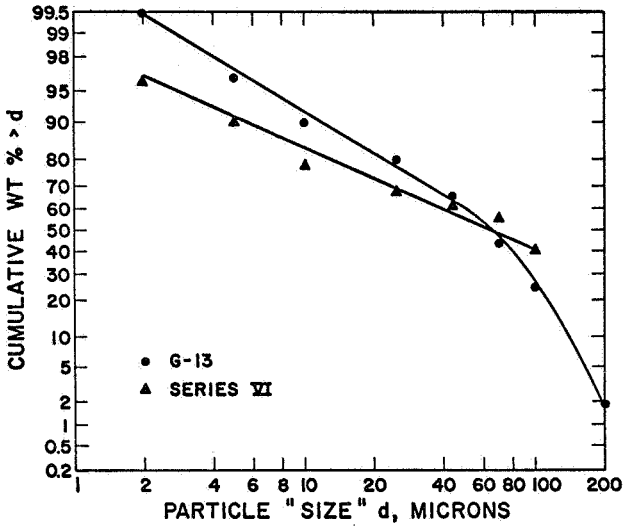

Fig. 5. Cumulative size distribution of -80 mesh fraction of Series VI final product (Grinds S+T+U) compared with that of Lot G-13 graphite flour.

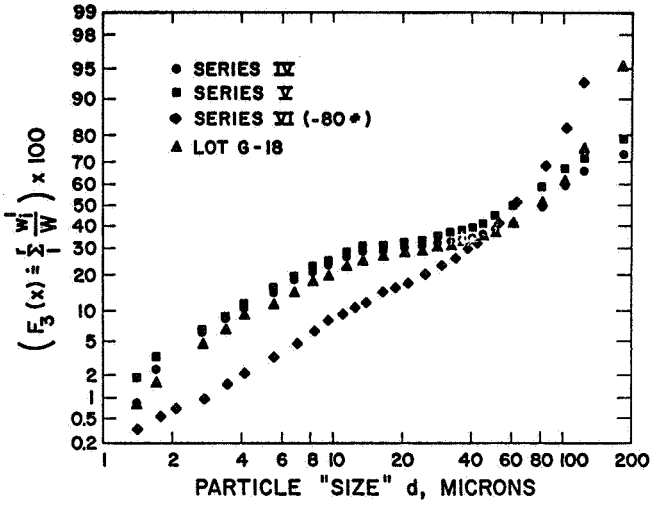

Fig. 6. Log-probability plots of Micromerograph "size" distribution data for three Santa Maria graphite grinding products and Lot G-18 graphite flour.

product contained an undesirably great proportion of +80 mesh material and too little -170+325 mesh material.

In Series V the initial hammer-milling was followed by two fluid-energy millings, the second with pressure on the opposing jet reduced to 50 psi. The effect of the second fluid-energy grind was small and was principally an increase in the proportion of -325 mesh fines, which was not desired.

For Series VI the grinding schedule was one hammer-milling using a relatively coarse discharge screen (S), a second hammer-milling using a moderately coarse screen (T), and fluid-energy milling with slightly reduced pressure (80 psi) on the opposing jet. The screen analysis of the final grinding product does not obviously resemble that of G-13 flour. However, Micromerograph analysis of the -80 mesh fraction of this product yielded a cumulative size distribution curve, plotted in Fig. 5, which did somewhat resemble that of Lot G-13. Except for a small proportion of material at the coarse end of the region plotted, the ranges of particle sizes and the slopes (variances) of the two distribution curves are similar. Accordingly, a larger lot -- about 12 lb. -- of the graphitized lump material was ground by the same schedule (S+T+U) used for Series VI, and was identified as Lot GP-14. Its screen analysis (Table II) was quite similar to that of the final Series VI product. To increase its resemblance to Lot G-13 it was screened through a 62-mesh SWECO sieve (which has ~300 μ openings, and so is approximately equivalent to a No. 50 U. S. Standard sieve) on a SWECO Vibro-Separator. The screen analysis of this -62 mesh product is also shown in Table II. Compared with Lot G-13 it still has a large excess of +80 mesh material and a large deficiency in the -170+325 mesh range. It is, however, lower in -325 mesh fines than was Lot GP-12, described above, and has also been used in extrusion experiments. The results of these experiments, discussed below, suggested the desirability of a particle-size distribution similar to that of GP-12 but with a proportion of fines intermediate between those of GP-12 and of the -62 mesh fraction of Lot GP-14. This was successfully produced as Lot GP-15 (Table II) by two stages of hammer-milling (S+T) and one of fluid-energy milling (I) using normal jet pressures.

Micromerograph analyses of three of the grinding products described above and of Lot G-18, another sample of Great Lakes Grade 1008-S graphite flour, are compared in Table III and Fig. 6. Because the Micromerograph is an air-sedimentation device in which settling rate is influenced by particle shape, it is not clear that the data shown are properly comparable. A blocky particle of Santa Maria

TABLE III

SUMMARY OF MICROMEROGRAPH "SIZE" DISTRIBUTION DATA

"Size" Interval, Microns	Weight % in "Size" Interval			
	Series IV	Series V	Series VI[a]	Lot G-18[b]
>200	~27	~21	~5	
200-100	14	12	35	~18
100-70	12	13	14	25
70-44	11	14	11	23
44-25	5	8	6	14
25-10	6	6	8	11
10-5	11	11	9	5.2
5-2	9	9	8	2.1
<2	4	5	3	0.7

(a) Minus 80 mesh fraction

(b) Great Lakes Grade 1008-S graphite flour

flour might be expected to have a sedimentation rate quite different from that of a flaky particle of 1008-S flour having equal volume, and so far there is no practical way to correct for particle shape. It is clear, however, that the log-normal description applies quite well to the 1008-S flour and very poorly to the Santa Maria flours. From these and other, similar plots it is also clear that the family of curves representing "size" distributions of ground Santa Maria coke or graphite is unusual principally in having a pronounced hump in the vicinity of 10 μ. This represents a large concentration of particles having about the dimensions of the optical domains observed microscopically, and apparently represents a natural size to which Santa Maria coke tends to break. As was reported in LA-4171-MS, the tendency to break to this size is very pronounced in the green coke, and less so in the calcined coke. The graphitized lump material appears to be intermediate in this regard. To approach the type of size distribution represented by 1008-S graphite flour it is probably advantageous to grind Santa Maria coke in the calcined condition. Some degree of control can probably be exercised by adjusting the calcining temperature. However, it now appears unlikely that a log-normal size distribution will be closely approached by grinding a Santa Maria filler in any condition.

D. Filler-Particle Packing Density (R. J. Imprescia)

The filler-particle packing densities listed in the last two columns of Table II are intended to indicate relative packing efficiencies of the particle distributions produced by the various grinding schedules. They are determined by molding a cylinder from a known weight of a given grinding product and dividing this weight by the volume of the cylinder produced. In one of the techniques used, stearic acid is added as a binder substitute, primarily to lubricate the relative motion of filler particles, and the cylinder is molded at low pressure and at a temperature just above the melting point of the acid. In the other technique a pitch binder is used and the cylinder is molded at the same pressure used in the stearic-acid method, which is maintained during slow heating to 900°C. Packed filler densities measured by the two techniques usually agree quite well. However, as is evident in Table II, this was not always true for ground Santa Maria fillers. The differences are believed to result from elastic springback of the compacted filler-particle network in the molding die following release of the molding pressure. Apparently the pitch-binder residue is strong enough to maintain coherence in the formed body during springback, while the stearic acid is not. Delamination cracks were observed in all of the stearic-acid specimens after removal from the die, and in most cases were plentiful enough to increase the bulk volume of the specimen significantly. In general, the coarser the filler the higher the crack concentration and the lower the apparent packing density. No cracks were detected in any hot-molded, pitch-bonded specimen, and the higher packing densities determined by this technique are believed to be correct.

Except for the coarsest filler investigated, the first grinding product of Series I, filler-particle packing densities measured by hot molding were essentially identical for all grinding products, independent of grinding schedule and particle-size distribution. They are not high enough to indicate extremely good particle packing, suggesting that the humped size distributions of the fillers investigated

TABLE IV

PROPERTIES OF HOT-MOLDED GRAPHITES MADE FROM SANTA MARIA FILLERS

Graphite Lot No.	Filler[a]	Mixing[b]	Bulk Density, g/cm^3		Electrical Resistivity, μΩcm		CTE x 10^{-6}/°C[c]		Anisotropy Ratios[d]			
									Crystalline		Electr.	Thermal
			Baked	Graph.	WG	AG	WG	AG	BAF	M	Resist.	Expansion
56 P-1	CP-6(900)	Dry	1.560	1.658	2150	2000	4.76	5.38	1.02	0.1	0.93	1.13
57 A-1	CP-6(900)	Solvent	1.628	---	1910	1975	6.36	6.06	1.03	0.32	1.03	0.95
57 B-1	CP-6(900)	Solvent	1.613	1.706	1920	1990	5.08	5.81	1.03	0.23	1.04	1.14
57 C-1	CP-6(900)	Solvent[e]	1.590	1.683	2200	2210	5.50	5.45	1.02	0.20	1.00	0.99
57 D-1,2	CP-6(900)	Solvent[g]	1.72	---	1750[f]	1450	5.28	5.88	1.04	0.35	0.83	1.11
57 D-3	CP-6(900)	Solvent[g]	1.74	---	1480	1450	5.42	5.27	1.01	0.28	0.98	0.97
56 Z-1	CP-10	Dry	1.563	1.591	1825	1710	5.06	5.02	~1.00	<0.1	0.94	0.99
57 E-1	CP-10	Solvent[g]	1.644	1.781	1440	1630	---	---	1.04	0.34	1.13	---
57 F-1	CP-10	Solvent[g]	1.684	1.761	1440	1550	5.47	6.06	1.02	0.29	1.08	1.11

(a) Fillers are described in Tables V and VI of LA-4171-MS.

(b) Mixing procedures are described on pp 19-20 of LA-4171-MS. Except in one case where acetone was used, the solvent-blending was tetrahydrofuran, "THF".

(c) Average coefficient of thermal expansion, 25-645°C.

(d) BAF = Bacon Anisotropy Factor, σ_{oz}/σ_{ox}. M = exponent in cosine function, $I(\Phi) = I_o \cos^M \Phi$, which best describes the change in concentration of basal planes with angle relative to the molding axis.

(e) Acetone solvent.

(f) This value may be in error.

(g) Hot mixed after solvent blending.

are not desirable when high final densities are required.

The springback behavior described above may be troublesome in forming graphite bodies from Santa Maria fillers. For example, during extrusion under high pressure, diametral springback in the green rod as it leaves the die may cause internal cracking since, at this stage, the filler particles are necessarily bonded together quite weakly.

E. Solvent-Blending (R. J. Imprescia)

Because of persistent difficulties in mixing the components of the pitch-bonded mixes used for hot-molding, a series of solvent-blending experiments was undertaken. The green mixes and blending procedures used were described in LA-4171-MS, together with some properties of the graphites produced. Additional properties have since been measured and are listed in Table IV, where they are compared with those of two otherwise similar graphites, Lots 56P-1 and 56Z-1, which were made using normal dry-blending procedures.

Microscopic examination of these graphites showed that solvent-blending had improved binder distribution and increased filler-particle wetting by the binder. The best structures were produced when solvent-blending was followed by hot-mixing, which was the case with Lots 57D-1 and 2, 57D-3, 57E-1, and 57F-1. Improvements in internal structure were reflected particularly in increases in bulk density and decreases in electrical resistivity. Use of acetone as the binder-solvent yielded an internal structure much like that observed when tetrahydrofuran was used, but produced a graphite having distinctly lower density and higher electrical resistivity.

TABLE V

MANUFACTURING DATA, EXTRUDED GRAPHITES MADE FROM SANTA MARIA FILLERS

Specimen No.	Filler Lot No.[a]	Mix Comp., Parts by Wt.			Extrusion Conditions				Green Dia, in.
		Filler	Thermax[b]	Binder[c]	Pressure, psi	Speed, in./min	Chamber Temp., °C	Mix Temp., °C	
ABX-1	GP-12	85	15	42.9	3400	160	48	74	0.5035
ABX-2	GP-12	85	15	35.7	6500	164	52	46	0.5035
ABX-3	GP-12	85	15	30.	14,400	156	48	42	0.5125
ABX-4	GP-12	100	0	39.7[e]	6500	160	48	44	0.509
ABY-1	GP-14[d]	85	15	30.0[e]	8100	160	49	46	0.5025
ABY-2	GP-14[d]	85	15	30.0	8550	156	48	45	0.5025
ABY-3	GP-14[d]	100	0	34.	6300	160	49	36	0.508

(a) Described in Table II and accompanying text.

(b) Thermax carbon black, Lot TP-4.

(c) Varcum 8251 furfuryl alcohol resin catalyzed with 4 wt % maleic anhydride.

(d) Minus 62 mesh fraction.

(e) Adjusted after first extrusion.

F. Extruded Graphites (J. M. Dickinson)

The ABX and ABY series of extruded graphites have been made from graphite flour produced by grinding Santa Maria coke which had been graphitized at 2700°C. With the exception of Lots ABX-4 and ABY-3, to which no carbon black was added, all were made using 85 parts Santa Maria graphite flour, 15 parts Thermax carbon black (Lot TP-4), and Varcum 8251 furfuryl alcohol resin binder catalyzed with maleic anhydride. All were extruded as 0.5-in. dia rods, under the conditions listed in Table V. Standard heat-treating cycles were used, with graphitization at 2840°C. Properties so far measured on these graphites are summarized in Table VI.

The ABX graphites were made from the graphite flour identified in Table II as Lot GP-12. Its screen analysis suggests a bimodal size distribution, with a very high proportion (55%) of -325 mesh fines. As would be expected from its content of fines, its binder requirement was very high. In spite of a particle-size distribution which appeared to be far from optimum, good graphites were produced. Densities were relatively high, elastic moduli were moderate and in the range to be expected of an isotropic graphite, and electrical resistivities were relatively low for the type of filler used. Lot ABX-1, containing the highest proportion of binder, had the highest density and modulus in the series, apparently because the yield of binder carbon was relatively high. However, fine cracks were found in several of the ABX-1 rods. Lot ABX-2 had similar properties and contained no detectable cracks. Lot ABX-3 was definitely deficient in binder, and it appears that a binder content of 35 to 37 pph may be optimum for this filler.

The ABY graphites were made using the -62 mesh fraction of Santa Maria graphite flour Lot GP-14 (Table II). Binder requirements were lower than for flour Lot GP-12, and 29 to 30 ppm of binder is probably optimum. Densities and elastic moduli were distinctly lower than for the better ABX graphites, indicating that the grinding schedule and size separation used in preparing flour GP-14 were not successful in improving its behavior as a filler.

As has usually been true, graphites made without carbon black were inferior in both density and elastic modulus to those made with additions of carbon black. However, even at lower densities, their electrical resistivities were distinctly less than when carbon black was present in the

TABLE VI

PROPERTIES OF EXTRUDED GRAPHITES MADE FROM SANTA MARIA FILLERS

Specimen No.	Condition	Bulk Density, g/cm^3	Binder Residue, %	Young's Modulus, 10^6 psi (a)	Electrical Resistivity, $\mu\Omega$ cm (a)
ABX-1	Cured		86.4±0.5		
	Baked		52.4±0.3		
	Graph.	1.876±0.01	51.0±0.3	1.97±0.04	1699±15
ABX-2	Cured	1.773±0.0005	84.9±0.1		
	Baked	1.777±0.002	48.3±0.07		
	Graph.	1.865±0.002	46.8±0.1	1.93±0.01	1639±6
ABX-3	Cured		85.9±0.2		
	Baked		46.7±0.1		
	Graph.	1.802±0.004	43.8±0.3	1.58±0.01	1876±22
ABX-4	Cured	1.801±0.002	85.6±0.3		
	Baked	1.761±0.003	47.6±0.2		
	Graph.	1.809±0.004	45.6±0.3	1.72±0.02	1470±12
ABY-1	Cured	1.803±0.003	85.6±0.5		
	Baked	1.748±0.008	47.0±0.6		
	Graph.	1.819±0.006	45.6±0.6	1.60±0.03	1668±9
ABY-2	Cured	1.801±0.002	85.6±0.3		
	Baked	1.753±0.002	47.4±0.2		
	Graph.	1.827±0.002	45.8±0.3	1.67±0.02	1665±16
ABY-3	Cured	1.772±0.004	83.9±0.5		
	Baked	1.717±0.007	41.8±0.4		
	Graph.	1.750±0.008	40.4±0.4	1.38±0.03	1484±30

(a) With-grain.

mix formulation.

G. Y-12 Sample of Santa Maria Coke (J. A. O'Rourke, R. D. Reiswig, L. S. Levinson)

A sample of Santa Maria LV coke, representing a lot received by the Y-12 Plant of Union Carbide Corporation during May, 1969, has been compared with the Santa Maria green coke purchased by CMF-13 in December, 1968, and the Santa Maria LV coke purchased by CMF-13 in January, 1969. The Y-12 sample was examined by optical and electron microscopy and by x-ray diffraction both as-received and after graphitizing for 1/2 hr at 2820°C. In both conditions, its microscopic appearance was essentially identical with those of the two CMF-13 lots after similar heat treatments. In the sections examined there may have been a slightly higher concentration of the typical rosette patterns in the Y-12 sample. This, however, was

not a clearcut difference, and some variation in concentration of this distinctive type of structural unit has been noted from lump to lump within the CMF-13 lots. X-ray parameters were:

	L_c (Å)	d_{002} (Å)
Y-12 Sample, LV coke, as-received	18.9	3.43
CMF-13 Sample, LV coke, as-received	19.7	3.42
CMF-13 Sample, green coke, calcined at 900°C	16.0	3.43
Y-12 Sample, LV coke, graphitized at 2820°C	320	3.370
CMF-13 Sample, green coke, graphitized at 2800°C	370	3.369

It appears that the Y-12 shipment of Santa Maria LV coke was essentially identical with the CMF-13 shipment of LV coke and also with the product of calcining the CMF-13 shipment of green coke. At least over a period of about six months the internal structure of Santa Maria coke shipped by Collier Carbon and Chemical Corporation has not changed significantly. Results of the CMF-13 investigations should apply directly to the material received by Y-12, and vice versa.

III. HIGHLY ORIENTED POLYCRYSTALLINE GRAPHITES

A. General

CMF-13 has undertaken development of a class of highly oriented polycrystalline graphites for possible use in a variety of applications in which the high degree of anisotropy potentially available in such a material can be used to advantage. This is expected to include nose-tips and heat shields for reentry vehicles, very high temperature piping, and certain kinds of nuclear reactor hardware. The CMF-13 program in this area was first described in LA-4057-MS, and subsequent work was summarized in LA-4128-MS.

From these preliminary investigations it was concluded that the most promising type of material for initial development was a hot-molded, pitch-bonded graphite made from natural flake graphite plus carbon black. Recent work has therefore been directed principally toward determining the optimum ratio of natural graphite to carbon black in such a filler.

B. Raw Materials

The principal filler material being used in this phase of the program is Southwestern Graphite Co. Grade 1651 natural graphite flakes, identified by CMF-13 as Lot G(Na)-21. This is a very fine filler (100% -325 mesh), with particle density of 2.272 g/cm^3. Chemical analysis by LASL Group CMB-1 showed that it contained 0.099% H_2O, 3.16% ash, 0.53% Fe, and 0.17% S. Most of its relatively high impurity content is eliminated by heat treatment at normal graphitizing temperatures.

The carbon black used is Thermatomic Carbon Co. Thermax carbon black, CMF-13 Lot TP-4. This is essentially identical with CMF-13 Lot TP-3, which was described in detail in LA-3872-MS and LA-3932-MS.

Barrett 30 MH pitch, a common coal-tar pitch produced by Allied Chemical Co., is used as binder. It is identified by CMF-13 as Lot PP-3. In the initial work described below an amount of extrusion oil equal to 5% of the weight of pitch was added to it as a lubricant, and was considered binder in the mix formulations and binder-residue calculations. It was subsequently concluded that this addition contributed nothing useful to binder behavior, and it was omitted from later members of the series.

C. Manufacturing Procedures (R. J. Imprescia)

In preparing all but two of these specimens, solvent-blending was used. The binder and extrusion oil were dissolved in tetrahydrofuran and the filler was added to the solution with mechanical stirring, which was continued until the mix became stiff enough to overload the mechanical stirrer. Thereafter mixing was continued by hand spatulation until a heavy, pasty consistency was produced. Then the mix was passed repeatedly through a heated food chopper to drive off any remaining solvent and in the

TABLE VII

MANUFACTURING DATA, HOT-MOLDED ANISOTROPIC GRAPHITES

Specimen No.	Mix Comp., Parts by Wt.			Calculated Binder Optimum, pph	Binder Residue, %		Density, g/cm^3				Dimensional Change, Baked to Graph., %	
							Bulk		Packed Filler			
	Filler[a]	Carbon Black[b]	Binder[c]		Baked	Graph.	Baked	Graph.	Baked	Graph.	$\Delta \ell$	Δd
59G-1	100	0	20	20.2	75.4	57.2	1.954	1.873	1.687	1.672	+1.0	-0.1
58E-1[g]	100	0	20	13.9	37.7	---	1.973	1.877	1.835	1.802	+1.6	+0.1
59A-2	95	5	23	18.5	51.5	37.4	1.926	1.858	1.713	1.704	+0.5	+0.0
59H-1[e]	95	5	18	17.2	60.9	43.4	1.934	1.860	1.742	1.725	+0.9	+0.0
59Hc-1[f]	95	5	18	17.2	49.9	32.3	1.901	1.829	1.744	1.728	+0.8	+0.1
59B-1	90	10	23	19.6	51.4	37.5	1.889	1.835	1.681	1.683	-0.0	-0.0
59J-2[f]	90	10	20	19.0	60.0	44.4	1.894	1.840	1.691	1.689	+0.1	-0.0
59Jb-1[f]	90	10	20	18.9	59.4	43.9	1.893	1.836	1.692	1.688	+0.2	0.0
59C-1	85	15	25	21.8	63.6	47.7	1.893	1.845	1.623	1.640	-0.0	-0.0
59K-1[f]	85	15	22	22.4	73.4	59.9	1.871	1.830	1.611	1.617	-0.2	-0.1
50B-1[d]	80	20	20				1.661	1.648			-1.4	-0.3
59D-2	80	20	25	20.7	55.6	---	1.871	1.822	1.633	---	---	---
59L-1[f]	80	20	22	22.6	70.9	57.6	1.846	1.820	1.597	1.615	-0.6	-0.2
59E-1	75	25	25	22.6	55.5	44.1	1.817	1.805	1.586	1.618	-1.3	-0.3
59F-1	70	30	28	27.9	56.6	46.2	1.729	1.740	1.482	1.532	-1.9	-0.7
59M-1[f]	70	30	28	24.7	61.1	51.1	1.799	1.795	1.537	1.570	-1.0	-0.6

(a) Natural graphite flakes, Lot G(Na)-21.

(b) Thermax, Lot TP-4

(c) Barrett 30MH pitch, Lot PP-4, plus 5% extrusion oil

(d) Previously reported. Specimen 4 in. dia x ~2.5 in. high,dry blended, molded at 1500 psi.

(e) Specimen 4 in. dia x ~1.25 in. high.

(f) Specimen 3 in. dia x ~1.25 in. high.

(g) Dry-blended.

expectation that the pitch would soften and hot-mixing would occur. With these formulations, however, after a few passes through the chopper, the still wet, spaghetti-like extrudate from the chopper became progressively more flaky and pressure in the chamber diminished. The mix appeared to have been fluidized, and the feeding screw turned quite freely in it. Hot chopping was not accomplished, although the chopping operations probably did improve mixing.

The first specimens in this series were hot-molded in 1.5-in. dia graphite dies, later ones in 3-in. or 4-in. dia graphite dies. Molding pressure was 4000 psi, which was maintained during heating at a constant rate to 900°C over a period of 18 hr. Graphitization was in flowing helium at approximately 2800°C.

Mixture compositions, densities, and shrinkages of these graphites are summarized in Table VII. Binder concentrations were estimated by the stearic-acid technique, and in most cases agreed quite well with the optimum binder contents subsequently calculated from the dimensions of

TABLE VIII

PROPERTIES OF HOT-MOLDED ANISOTROPIC GRAPHITES[a]

Specimen No.	Percent Carbon Black	Bulk Density g/cm^3	Young's Modulus, 10^6 psi		Strength, psi						CTE[b] x 10^{-6}/°C		Thermal Conductivity W/cm-°C		Electrical Resistivity μΩcm	
					Tension		Compression		Flexure							
			WG	AG	WG	AG	WG	AG	WG	AG	WG	AG	WG	AG	WG	AG
59G-1	0	1.87									1.79	11.35			630	3920
58E-1	0	1.88									1.09	15.74			490	7025
59A-2	5	1.86									1.57	9.40			720	3525
59H-1	5	1.86	3.18	0.63	2500	~870[c]	4910	7310	4890	1700	1.93	10.4	1.79	0.43	850	3600
59Hc-1	5	1.82	3.00	0.58	2570	~860[c]	5230	7100	4725	1590	1.77	10.9	1.60	0.38	830	3380
59B-1	10	1.84									1.45	8.95			760	3700
59J-2	10	1.84	2.75	0.66	2330	~970[c]	5330	7260	4630	1930	---	10.0	1.54	0.45	940	3250
59Jb-1	10	1.83	2.83	0.64	2360	~810[c]	5430	8060	5300	1815	1.81	8.92	1.63	0.45	900	3430
59C-1	15	1.85													790	3870
59K-1	15	1.83														
50B-1	20	1.65	2.90	2.00	2590	1050[d]	4810	7100	5440	1790	1.18	9.32	1.27	0.25	880	5390
59D-2	20	1.82									2.13	9.14			910	3700
59L-1	20	1.82														
59E-1	25	1.81													990	3780
59F-1	30	1.74									2.26	7.74			1280	3850
59M-1	30	1.80														

(a) WG = With-grain, AG = across-grain.

(b) Average coefficient of thermal expansion, 25-645°C.

(c) Estimated from with-grain tensile strength and anisotropy of flexural strength.

(d) Previously reported as 1556. This value was not duplicated in subsequent tests.

the hot-molded specimens. Binder residues in the baked condition were unusually high, in one case exceeding 75% (compared with 50% or less in most hot-molded materials). Binder residues were much lower after graphitization, although an appreciable part of the loss was actually vaporization of impurities from the filler rather than loss of volatiles from the binder, as is assumed in the calculation of binder residue.

Bulk densities in the baked condition were generally high. That of Specimen 59F-1, which had the highest carbon-black content in the series, increased slightly on graphitization. All other specimens decreased slightly in bulk density upon graphitization. In no case did packed filler density change significantly, indicating that most of the change in bulk density resulted from volatilization of binder residues and filler impurities. Carbon-black contents up to perhaps 20% apparently stabilized the filler network against dimensional changes during graphitization. At still higher carbon-black concentrations there was appreciable shrinkage during graphitization.

D. Properties

Properties so far collected on these graphites are listed in Table VIII and anisotropy ratios in Table IX. It appears that up to at least 10% and perhaps to 15% carbon black in the filler there are no large changes in measured properties or anisotropies of the graphites produced.

TABLE IX

ANISOTROPY RATIOS, HOT-MOLDED ANISOTROPIC GRAPHITES

Specimen No.	Percent Carbon Black	Crystalline Anisotropy BAF[a]	Crystalline Anisotropy M[b]	Young's Modulus	Tensile Strength	Compressive Strength	Flexure Strength	Thermal Expansion	Thermal Conductivity	Electrical Resistivity
59G-1	0	3.56	6.4					6.34		6.23
58E-1	0	4.11	9.8					14.44		14.25
59A-2	5	2.94	5.5	---				5.99		4.88
59H-1	5	---		5.05	(c)	1.49	2.88	5.39	4.16	4.22
59Hc-1	5	2.82	5.3	5.14	(c)	1.36	2.97	6.16	4.21	4.07
59B-1	10	2.96	5.6					6.17		4.84
59J-2	10			4.16	(c)	1.36	2.40		3.42	3.46
59Jb-1	10	2.85	5.0	4.40	(c)	1.49	2.92	4.93	3.62	3.81
59C-1	15	2.78	5.3							4.90
50B-1	20			1.45	2.46	1.48	3.04	7.90	5.08	6.14
59D-2	20	2.56	5.2					4.29		4.05
59E-1	25	2.18	4.2							3.83
59F-1	30	1.72	3.4					3.42		3.00

(a) Bacon Anisotropy Factor, σ_{oz}/σ_{ox}.

(b) M is the exponent in the cosine function, $I(\Phi) = I_o \cos^M \Phi$, which best describes the change in concentration of basal planes with angle relative to the molding axis.

(c) Assumed to be the same as for flexure strength.

(This, however, may not be true of permeability, which has not been investigated.) Results for specimens 58E-1 and 50B-1 are anomalous. Both were dry-blended instead of solvent-blended, but have good properties and unusually high anisotropy ratios. A relatively high across-grain tensile strength previously reported for 50B-1 was not repeated in additional tests on specimens cut from the same molded cylinder. This specimen was also unusual in showing lower anisotropy of tensile strength than of flexure strength, which has not been the case for most other graphites tested by CMF-13 or reported in the literature. In general the ratio of tensile to flexure strength has been found to vary over a rather wide range, but anisotropy ratios for the two types of strength measurements have usually agreed quite well.

Microscopically, several of these graphites showed evidence of poor mixing in the form of lenticular volumes of undistributed binder residue, sometimes containing visible porosity. With increasing carbon black content the degree of preferred orientation of the flaky filler particles decreased continuously, and perhaps more rapidly than would be expected from the x-ray parameters listed in Table IX.

E. Extruded Highly Oriented Graphites (J. M. Dickinson)

For such applications as reactor tubes and high-temperature piping, it appears desirable to produce highly anisotropic polycrystalline graphites in extruded shapes in which the layer structure of the graphite is oriented preferentially parallel to surfaces of the extrusion. The development of graphites of this type has begun with extrusion of two lots of material in which the principal filler was the natural flake graphite described above, Lot G(Na)-21. In both cases this was mixed with Thermax

carbon black, Lot TP-4, in the proportion 85 parts flake graphite to 15 parts Thermax. For extrusion Lot ABZ-1 the binder was 57 pph of Varcum 8251 furfuryl alcohol resin catalyzed with maleic anhydride. For Lot ABZ-2 it was 60 pph of Barrett 30 MH pitch, Lot PP-3. Both were extruded as solid rods, Lot ABZ-1 as 1/2-in. dia rounds and Lot ABZ-2 as 5/8-in. dia rounds.

Presumably because of the extreme fineness and large surface area of the natural graphite flakes, binder requirements for extrusion were very high. Extrusion pressures were very low, and it was necessary to extrude at low rates to produce sound-appearing rods. The green rods of Lot ABZ-1, bonded with furfuryl alcohol resin, had a somewhat laminar surface appearance. Surfaces of the pitch-bonded rods, Lot ABZ-2,were good. Both lots survived baking and graphitizing, but after graphitization both showed end cracks representing internal separations parallel to the oriented natural graphite flakes. Lot ABZ-1 showed high shrinkage and fine end cracks. For Lot ABZ-2 shrinkage was less and cracks were larger and more numerous. Both graphites were highly anisotropic.

To produce sound, highly oriented, extruded graphites of this type it will probably be necessary both to reduce binder requirement and to increase extrusion pressure. Other binders will be tried, but an adjustment of particle-size distribution may be required.

IV. GRAPHITE FILLER MATERIALS

A. Grinding Research (R. J. Imprescia, H. D. Lewis)

A study of the grindability of a needle coke as a function of feed rate to a Trost fluid-energy mill was summarized in LA-4128-MS. Grindability was expressed in terms both of relative fineness of the ground product (P_F, in grams of -10 μ fines produced per minute) and of relative surface area (P_P, in square meters of new surface area produced per minute, measured by the permeability method). More recently the HB series of grinding products, produced by grinding an intermediate size fraction of the needle coke, has been examined for surface area by the BET (nitrogen-adsorption) method. Grindabilities

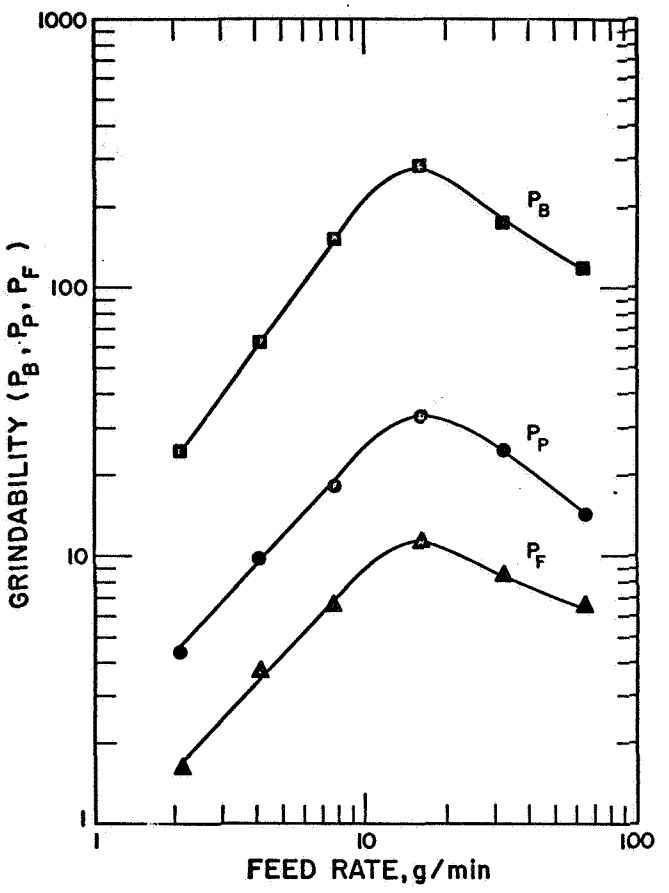

Fig. 7. Trost-mill grindabilities as functions of feed rate for the intermediate size-fraction of needle coke (HB series).

calculated from BET surface areas (P_B, m^2/min) are plotted as a function of feed rate to the mill in Fig. 7, together with data previously reported for P_F and P_P.

As was true of grindabilities calculated from the other two types of measurements, P_B increases about linearly with feed rate to a maximum value near 15 g/min, then decreases at higher feed rates. However, while the P_P and P_F curves have slopes of approximately 1.0 up to the maximum, the slope of the P_B curve is about 1.4. In all grindability studies so far done here, a difference of this type has appeared. Grindabilities calculated from size analysis (P_F) and from surface area indicated by a permeability measurement (P_P) have usually agreed quite well, and have differed from that determined by BET surface-area measurements (P_B). Table X suggests a reason for this difference.

TABLE X

PARTICLE CHARACTERISTICS, TROST-MILLED NEEDLE COKE (HB SERIES)

Grind No.	Feed Rate, g/min	Micromerograph Sample Statistics[a]								BET Surface Area		Fuzziness Ratio
		$\hat{\mu}_{x3}$	$\hat{\sigma}^2_x$	$\hat{\mu}_x$	$\bar{d}_3$ microns	$\bar{d}$ microns	s^2_d	S_W M^2/g	CV_d	S_W M^2/g	d_s[b] microns	R_F[c]
HB-1	2.1	1.8452	0.54111	0.2219	8.296	1.636	1.922	0.5833	0.847	12.707	0.22	21.78
HB-2C	4.1	1.7259	0.47389	0.3042	7.119	1.718	1.789	0.6355	0.779	16.237	0.17	25.55
HB-3A	7.7	1.7831	0.51402	0.2411	7.691	1.646	1.820	0.6123	0.820	20.584	0.14	33.62
HB-4A	16.0	1.9435	0.61556	0.0968	9.499	1.499	1.910	0.5488	0.922	18.832	0.15	34.31
HB-5	31.9	3.5773	2.5968	-4.2130	131.07	0.0542	0.0365	0.2884	3.524	6.481	0.44	22.47
HB-6	64.2	4.7456	3.3797	-5.3936	623.59	0.0246	0.0172	0.1404	5.326	2.804	1.00	19.97

(a) Based on log normal model.

(b) $d_s = 6/\rho S_W$ = diameter of smooth-shelled sphere having specific surface area equal to that measured by BET method.

(c) $R_F = S_W$ (BET)/S_W (Calc.) = ratio of specific surface area measured by BET method to that calculated from Micromerograph sample statistics assuming smooth-shelled spheres.

The values of specific surface area, S_W, listed in Column 9 of Table X are calculated from Micromerograph particle-size analyses of the grinding products, with the assumption that all particles are smooth-shelled spheres. The values of S_W in Column 11 are those measured directly by the BET method. The "Fuzziness Ratios" in the last column compare these two sets of values, and so indicate relative roughness of the particle surfaces. With increasing feed rate to the mill the fuzziness ratio at first increases, suggesting an increase in surface roughness or in surface-connected porosity, and then decreases, suggesting production of relatively smooth, pore-free particles. The BET measurement, then, includes an increment of area (representing surface roughness or surface-connected porosity) which does not affect overall particle dimensions. Evidently it also does not significantly affect the permeability of a bed of particles to gas flow through the bed. The greater slope of the first part of the P_B curve of Fig. 7 is, then, explained by an increasing increment of area of the type represented by an increasing fuzziness ratio. Since production of this type of new surface necessarily absorbs grinding energy, an argument can be made that the P_B curve is a better representation of relative grindabilities than are the P_p and P_F curves.

B. Mixed Fillers (R. J. Imprescia)

Two widely different filler materials which have been investigated by CMF-13 are Lot G(Na)-21, the fine natural flake graphite described above, and Lot G(HCTE)-23, a "secondary" graphite flour made by Union Carbide Corporation by grinding a pitch-bonded graphite made from its experimental high-CTE (coefficient of thermal expansion) Robinson coke. The natural graphite particles are very flaky and highly graphitic, while those of the high-CTE graphite are blocky, nearly equiaxed, and have a very fine, random internal structure.

Hot-molded graphites have been made from these two flours and from mixtures of them in various proportions. Binder requirement was estimated by the stearic-acid technique to be about 20 pph for all of these fillers and, in the manufacture of hot-molded specimens, Barrett 30 MH pitch binder (Lot PP-3) was used in this proportion in all mix formulations. All blending was done as dry powders. Molding pressure was 4000 psi, which was maintained during heating to 900°C at a constant rate over

TABLE XI

MANUFACTURING DATA, HOT-MOLDED GRAPHITES MADE FROM MIXED FILLERS

Specimen No.	Mix Comp., Parts by Wt. Filler G(HCTE)-23	Filler G(Na)-21	Pitch Binder	Calculated Binder Optimum, pph	Binder Residue (Baked) %	Density, g/cm^3 Bulk Baked	Bulk Graph.	Packed Filler Baked	Packed Filler Graph.	Dimensional Change, Baked to Graph., % $\Delta\ell$	Δd
58A-1	100	0	20	19.8	44.4	1.756	1.743	1.611	1.603	+0.7	-0.1
58B-1	75	25	20	17.4	42.8	1.828	1.843	1.684	1.711	-2.3	+0.2
58C-2	50	50	20	10.7	17.1	1.935	1.850	1.869	1.819	+1.7	+0.5
58D-1	25	75	20	12.8	33.4	1.959	1.873	1.836	1.796	+1.6	+0.3
58E-1	0	100	20	13.9	37.7	1.973	1.877	1.835	1.802	+1.6	+0.1

a period of 18 hr. Graphitization was in flowing helium at 2810°C.

Mixture compositions, binder data, densities, and shrinkages during graphitization are summarized for this series of graphites in Table XI. Especially for fillers containing a high proportion of graphite flakes, the stearic-acid technique consistently overestimated the binder requirement. (This is apparently because, in hot-molding, the natural graphite deformed to accomodate to the shapes of adjacent particles, thus filling interparticle voids which were occupied by stearic acid when the original estimate was made.) Squeezeout of excess binder contributed to the low values of binder residue shown in the table. Except for 58B-1, all specimens expanded and decreased in density during graphitization. Packed filler densities were extremely high.

Properties measured on these graphites are listed in Table XII. Bulk densities and anisotropies are plotted as functions of filler composition in Fig. 8. Bulk density of the graphitized specimen increases considerably with the first addition of flake graphite to the high-CTE filler, and thereafter increases slowly at a nearly constant rate. Anisotropy, particularly as represented by the Bacon anisotropy factor, increases slowly with the first flake graphite additions, and then much more rapidly. For this series of graphites, the agreement of electrical-resistivity and thermal-expansion anisotropies was remarkably close.

There appears, from these experiments, to exist a general possibility of using small additions of natural flake graphite to increase density, electrical conductivity, etc., without greatly increasing anisotropy of the finished graphite. This is now being explored further using a Santa Maria graphite flour as the principal filler material.

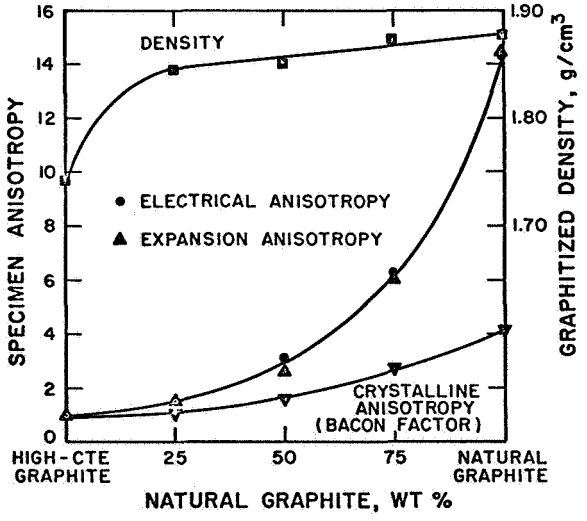

Fig. 8. Bulk density and anisotropy ratios as functions of filler composition for mixtures of high-CTE and natural graphite flours.

TABLE XII

PROPERTIES OF HOT-MOLDED GRAPHITES MADE FROM MIXED FILLERS[a]

Specimen No.	Percent G(Na)-21 in Filler	Bulk Density, g/cm^3	Electrical Resistivity, μΩcm		Coeff. of Thermal Exp.[b], x 10^{-6}/°C		Anisotropy Ratios			
							Crystalline		Electr. Resist.	Thermal Exp.
			WG	AG	WG	AG	BAF[c]	M[d]		
58A-1	0	1.743	1600	1680	6.54	6.95	~1.00	<0.1	1.05	1.06
58B-1	25	1.843	1330	1980	5.23	8.06	1.13	0.90	1.49	1.54
58C-2	50	1.850	1010	3160	3.53	9.10	1.63	2.80	3.12	2.58
58D-1	75	1.873	810	5050	2.03	12.22	2.74	5.3	6.21	6.02
58E-1	100	1.877	490	7025	1.09	15.74	4.11	9.8	14.25	14.44

(a) WG = with-grain, AG = across-grain.

(b) Average, 25-645°C.

(c) Bacon Anisotropy Factor, σ_{oz}/σ_{ox}.

(d) Exponent of the cosine function, $I(\Phi) = I_o \cos^M \Phi$.

V. GRAPHITE BINDERS

A. Molecular Compositions of Furfuryl Alcohol Resins (E. M. Wewerka)

Firm identifications have now been made of the low-molecular-weight products isolated from an acid-polymerized furfuryl alcohol resin by vacuum distillation and gas chromatography. They are: furfuryl alcohol, difurylmethane, difurylether, furfuryl alcohol dimer, and the next higher homolog of difurylmethane. Partial identifications have been made of species isolated from an alumina-polymerized resin and a furfuryl alcohol-formaldehyde copolymer. The tentative identification of a product isolated from the alumina-polymerized resin as a levulinic ester was apparently incorrect, but no alternative identification has yet been made. Two unique species have been separated from the copolymer resin, and are now being studied by mass spectrometry.

B. Alumina-Polymerized Furfuryl Alcohol Resins (E. M. Wewerka)

An investigation is in progress of the feasibility of polymerizing furfuryl alcohol by distilling it into a reflux column packed with γ-alumina catalyst, causing polymerization to take place in the column. This should result in efficient conversion of low-molecular-weight species -- particularly the monomer -- to higher molecular weights without producing enough of the very high molecular weight products to increase resin viscosities excessively. The catalyst beads used were made by Alcoa for the special purpose of polymerizing furfuryl alcohol, and are no longer manufactured.

A number of practical problems remain to be solved. However, gel permeation chromatography analyses of a few samples of resin made by this column-reflux method indicate that the desired result is being achieved.

C. Large-Scale Thermogravimetric Analysis (E. M. Wewerka, J. M. Dickinson)

An attempt has been made to correlate manufacturing behavior with small-scale differential thermal analysis results by means of full-scale thermogravimetric analyses of a group of 1/2-in. dia extruded graphite rods. The rods were made by standard techniques using a graphite flour filler and the following binders: Varcum 8251; EMW 238, a furfuryl alcohol-formaldehyde copolymer with viscosity of 600 cp; EMW 237, an acid-polymerized furfuryl alcohol resin, 850 cp; EMW 222, a γ-alumina polymerized furfuryl alcohol resin, 1200 cp; and a standard furfuryl alcohol re-

sin (EMW 232, 8400 cp) diluted with another furfuryl alcohol resin of much lower viscosity (EMW 236, 200 cp). The extruded rods were cured by heating in air at 2.5°C/hr. At a series of increasing temperatures one rod of each type was removed from the oven, weighed, and inspected visually.

All rods survived heating through the 150-200°C region, where intense thermal activity is indicated by differential thermal analysis, with small weight losses (9-14% of binder weight) and without cracking. Weight loss was about linear with temperature to 300°C, where typically 20-25% of the binder weight had been lost. At higher temperatures the rate of weight loss increased, and at 400°C about 40-50% of the binder weight had been lost. The experiment was discontinued at 400°C because the rods fell apart when they were removed from the oven. This is approximately the temperature of an exothermic peak observed for all of these resins by differential thermal analysis.

Samples removed from the oven at or below 350°C could be returned to the oven and baked to 450°C or 900°C without apparent damage, and could then be handled and appeared to behave in an ordinary manner.

Some differences were observed in the thermogravimetric behaviors of the various resin types. However, they were not of the magnitude which would be expected if weight loss were a direct manifestation of thermal behavior. Much more work will be needed before the observed behaviors can be understood. It is evident, however, that the furfuryl alcohol resin reactions which have been detected below 200°C by differential thermal analysis become relatively unimportant in the behavior of this type of resin as a binder if heating rates are kept below about 5°C/hr. It is also evident that graphites bonded with furfuryl alcohol resins become very fragile in the vicinity of 400°C during initial heating under the conditions used here.

D. Oxidation During Heat Treatment (J. M. Dickinson)

Damage to resin-bonded graphites has been reported to occur at temperatures in the vicinity of 400°C during long heat-treating cycles, either from the decomposition reactions considered above or from oxidation. To determine the relative importance of the two types of reactions, four identical graphites (the ABV series) were made, and two rods of each were treated in various ways. The graphites were extruded as 1/2-in. dia rods from a mix containing 85 parts Lot G-18 graphite flour, 15 parts Lot TP-4 Thermax carbon black, and 27 parts Varcum 8251 furfuryl alcohol resin.

Green rods heated from room temperature to 400°C in 160 hr in flowing helium were sound and had good surfaces. Rods similarly heat treated in flowing air exfoliated and were badly damaged on all surfaces, indicating that serious oxidation can occur during long heat treatments in this region of temperatures. Rods covered with Thermax carbon black, wrapped in aluminum foil, and heated in still air were protected from oxidation and had good surfaces. However, from previous observations it appears that the protection is borderline during slow cycles to 420°C or so, and that an improved procedure is desirable for long curing cycles at relatively high temperatures.

Six rods were packed in Thermax, covered with foil, cured to 200°C in 72 hr, and cooled to room temperature. Two of them were removed and heated in vacuum to 900°C; two were heated in still air to 400°C, removed, cooled, and heated in vacuum to 900°C; two were heated in still air to 420°C and then in vacuum to 860°C. All had satisfactory surfaces and essentially the same densities, carbon residues, and Young's moduli as did samples heat treated in flowing helium.

Although graphites bonded with furfuryl alcohol resins are fragile in the vicinity of 400°C until curing is completed, they are apparently not directly damaged by the curing reactions themselves. They can be damaged by oxidation during long heat treatments in this temperature region. The protection offered by packing in carbon black and covering with aluminum foil is effective to at least 200°C but apparently is not always adequate at 400°C. Heat treatment in flowing helium or in vacuum offers complete protection to still higher temperatures with no significant effect on densities or binder residues. However, to avoid excessive loss of low molecular weight binder components in the early stages of curing, heat treatment in vacuum should be preceded by precuring to perhaps

200°C in another environment.

E. Phenolic and Epoxy Binders (J. M. Dickinson, E. M. Wewerka)

The ABT series of graphites has been made using 85 parts Lot G-18 graphite flour, 15 parts Lot TP-4 Thermax carbon black, and 27 parts of one of the following resins: Plyophen 23-039, a furane-modified phenolic; Plyophen 23-029, a temperature-resistant phenolic (which was incorrectly listed in LA-4171-MS, page 28, as Plyophen 23-239); and Epotuf 37-140, a general-purpose epoxy resin. The room-temperature viscosity of Plyophen 23-039 is 3300 cp, that of Plyophen 23-029 is 220 cp, and that of Epotuf 37-140 is 14,000 cp.

Two specimens 1.5 in. dia and 0.5 in. high were made using each of these binders, by pressing at room temperature and 8500 psi. The specimens were cured and baked in cycles normally used for resin-bonded graphites, and graphitized at 2840°C. Specimen ABT-1, made from Plyophen 23-029, had a relatively high carbon residue (55.1%) but with relatively low density (1.604 g/cm^3), apparently because of large springback (0.021 in. on the diameter) upon removal from the die. Specimen ABT-4, made from Epotuf 37-140, had the opposite behavior; carbon residue was very low (25.8%) but there was little springback so that final density was 1.582 g/cm^3. Specimen ABT-2, made from Plyophen 23-039, was intermediate in both regards, with carbon residue of 48.5% and density of 1.632 g/cm^3. Duplicates of the three samples (ABT-5, ABT-6, and ABT-7) behaved similarly. Although densities were low in all cases, carbon yields from the two phenolic resins were high enough to be interesting. Therefore, a few extrusions were attempted.

Plyophen 23-029 requires no catalyst, and none was used. However, during the first series of five food choppings made to complete mixing and condition the mix, the heat and pressure developed were apparently enough to initiate polymerization -- although the maximum mix temperature reached was only 42°C. The mix "dried out" and stiffened during chopping, and polymerized in the extrusion press to the extent that it could not be extruded at maximum press pressure. However, a 2-in. dia billet made from material in the press chamber -- and identified as Lot ABT-8 -- was heat-treated successfully and had a graphitized density of 1.845 g/cm^3. Although it contained no macroscopic cracks, microscopic examination revealed the presence of many microcracks about 50 to 200 μ long both within the binder residue and along its interfaces with filler particles.

A second lot of the Plyophen 23-029 mix was prepared using only one chopping pass, and was identified as Lot ABT-10. This was extruded successfully as 0.5-in. dia rod at a rate of 116 in./min under pressure of 20,000 to 22,000 psi. Graphitized density was only 1.747 g/cm^3, showing the effect of inadequate mixing. Carbon residue was 49.7%, and Young's modulus was 1.63 x 10^6 psi.

Lot ABT-9 was made using catalyzed Plyophen 23-039 resin. It was chopped twice and extruded successfully, although extrusion pressure was very high (24,000) and extrusion rate very low (1.5 in./min). Graphitized density was 1.815 g/cm^3, carbon residue was 49.7%, and Young's modulus was 2.06 x 10^6 psi. In this case the high extrusion pressure probably resulted from the high initial viscosity of the resin (33,000), whereas in the case of Lot ABT-10 it apparently resulted from polymerization during extrusion of a resin whose initial viscosity was relatively low (220 cp).

F. Effects of Binder Chemistry (J. M. Dickinson, E. M. Wewerka, R. D. Reiswig, J. A. O'Rourke)

Two series of graphites, the ABU and ABW series, have been made to investigate the effects of binder chemistry upon graphitization and properties of resin-bonded graphites.

Series ABU consisted of three extrusions, in two of which formaldehyde was added directly to the binder. The filler used, CMF-13 Lot G-18, was a well-graphitized flour which was expected to interfere with observations of the degree of binder graphitization, but which has previously been used to produce many other graphites to which this series might be compared. Extrusion conditions are summarized in Table XIII, and properties of the finished graphites in Table XIV. During these three runs difficulty was experienced with the vacuum system which evacuates

TABLE XIII

MANUFACTURING CONDITIONS, ABU AND ABW GRAPHITES

Lot No.	Binder					Extrusion Conditions			
	Identification	Type	Additions	Viscosity, cp	Amount, %	Pressure, psi	Speed in./min.	Temp., °C	Green Dia., in.
ABU-1	Varcum 8251	Commercial PFA[a]	None	250	27[c]	5400	164	47	0.504
ABU-2	Varcum 8251	Commercial PFA[a]	1% HCHO[b]	≈250	27[c]	6975	164	48	0.5035
ABU-3	Varcum 8251	Commercial PFA[a]	5% HCHO	≈250	27[c]	6840	167	48	0.5055
ABW-1	EMW 221	Alumina-polymerized	None	6180	32.5		(cast)		
ABW-2	EMW 229	Alumina-polymerized	None	60	41.7		(cast)		
ABW-3	EMW 235	Acid-polymerized	None	300,000	30.3		(cast)		
ABW-4	EMW 236	Acid-polymerized	None	200	34.4		(cast)		
ABW-5	EMW 238	HCHO copolymer	None	630	30.8		(cast)		
ABW-6	EMW 198	HCHO copolymer	None	32,000	29.5		(cast)		
ABW-7	EMW 236	Mixed	1% para HCHO	≈200	32.5		(cast)		
ABW-9	EMW 236	Mixed	5% para HCHO	≈200	39.9		(cast)		

(a) PFA = polyfurfuryl alcohol = furfuryl alcohol resin.

(b) HCHO = formaldehyde.

(c) Including maleic anhydride polymerization catalyst, 4% of binder weight.

TABLE XIV

PROPERTIES OF ABU-SERIES GRAPHITES

Lot No.	Density, g/cm^3	Binder Carbon Residue, %	Electrical Resistivity μΩcm[a]	Young's Modulus 10^6 psi[a]	Crystallite Parameters		Crystalline Anisotropies[b]	
					L_c, Å	d_{002}, Å	M	BAF
ABU-1	1.855	45.9	1188	2.40	470	3.360	1.83	1.488
ABU-2	1.868	46.7	1148	2.47	440	3.359	1.86	1.496
ABU-3	1.847	45.5	1201	2.40	440	3.359	2.15	1.495

(a) With-grain properties.

(b) BAF = Bacon anisotropy factor, σ_{ox}/σ_{oz} ; M = exponent of sine in sine function which best represents angular distribution of reflected x-ray intensities.

the materials chamber of the extrusion press, and vacuum in the chamber was not as good as usual. Gases left in the charge are believed to explain the relatively large diameters of the green extruded rods, and the relatively low densities of the finished graphites. However, there was no indication that additions of either 1% or 5% formaldehyde to the furfuryl alcohol resin binder had a significant effect on the behavior or properties of the finished graphite. The microstructures of the three graphites were very similar, showing a high degree of preferred orientation of filler particles and no gross defects. It appeared that there might be an increase in porosity,

TABLE XV

X-RAY PARAMETERS OF SCREEN FRACTIONS, ABW GRAPHITES

Lot No.	Screen Fraction	Estimated Wt. % Binder Residue in Fraction [a]	L_c, Å	d_{002}, Å
ABW-1	-120 mesh	80	590	3.362
ABW-2	-120 mesh	70	700	3.360
ABW-3	-120 mesh	80-90	770	3.362
ABW-4	-120 mesh	70-80	640	3.363
ABW-5	-120 mesh	80-90	600	3.364
ABW-6	-120 mesh	80	770	3.359
ABW-7	-120 mesh	70-80	710	3.361
ABW-9	-120 mesh	70-80	720	3.362
Typical	-70+120 mesh	Very small	29	3.425

(a) Estimated by optical microscopy.

particularly in the larger sizes, with increasing formaldehyde content, accompanied by a tendency of the binder residue to etch darker. However, the differences -- if any-- were small. Crystallite parameters were nearly identical for the three materials, and x-ray measurements showed the same high degree of preferred orientation indicated by microscopic examination.

Series ABW included eight graphites made from the six furfuryl alcohol resin binders and the two copolymer resins listed in Table XIII. These binders cover a wide range of type and viscosity, and were expected to differ considerably in graphitizability. To facilitate determination of the degree to which they did graphitize, they were mixed with a narrow size fraction (-70+120 mesh) of a ground vitreous carbon, which was not expected to change significantly in internal structure during heat treatment. The mixes were cast, heat-treated in normal cycles, and graphitized at 2800°C. The graphitized pieces were crushed very gently -- to minimize comminution of the vitreous carbon filler particles -- to pass a 70 mesh sieve, and then were screened on a 120 mesh sieve. Optical microscopy confirmed that the -70+120 mesh fraction consisted almost entirely of essentially unaltered vitreous carbon filler, and that an estimated 70 to 90% of the -120 mesh fraction was well-graphitized binder residue. The binder residue in all cases showed well-developed lamellar structures and a high degree of optical anisotropy. Its highly graphitic nature was confirmed by x-ray measurements, which gave the parameters listed in Table XV. No significant difference was observed in the degree of graphitization reached by any one of these very dissimilar binders. The expected effects of molecular distribution and formaldehyde additions on the graphitizability of furfuryl alcohol resin binders have not yet been detected. However, strong effects of the filler on their graphitization have been demonstrated.

As was reported in LA-4171-MS, one sample of Varcum 8251 furfuryl alcohol resin and three experimental furfuryl alcohol-formaldehyde copolymer resins were cast, cured, baked, and graphitized, with no filler particles present. The highest heat-treating temperature then reported was 2800°C. They have since been heat-treated for 1/2 hr at 3000°C, again with little change in internal structure. The major component in all cases is still a highly cross-linked "non-graphitizing" carbon with crystallite size (L_c) of about 27 to 30Å and interplanar spacing (d_{002}) of 3.42 to 3.43Å. An ordered minor component with interplanar spacing of about 3.35Å appears to have increased

in amount as a result of this heat treatment, to an estimated 7 to 12% in the various samples. A turbostratic minor component with interplanar spacing of about 3.41Å is still present to the extent of about 5% in one of the copolymer samples, but has nearly disappeared from the other samples.

In the complete absence of a filler, the furfuryl alcohol and furfuryl alcohol-formaldehyde copolymer resins appear to be essentially nongraphitizable. In the presence of a nongraphitizing (vitreous carbon) filler they all graphitize very well, and to about the same degree. Their behavior in the presence of carbon blacks and of graphitic filler particles has not yet been fully examined because of interference of these filler materials with x-ray diffraction measurements on the binder residues.

VI. HIGH-TEMPERATURE MECHANICAL PROPERTIES

(W. V. Green, E. G. Zukas)

A. Evaluation of Back-Stresses Created by Creep Strain

As was first reported in LA-4171-MS, a series of experiments is in progress intended to evaluate the back-stresses created in graphite by creep strain. Fourteen tests have so far been made on ZTA graphite specimens extended either 2% or 10% in tensile creep at 2500°C under a unit load of 3200 psi. The tests are made by partially unloading the specimen after the desired amount of creep strain has occurred and observing its subsequent strain-recovery behavior. If positive creep continues, it is assumed that the externally applied unit load which the specimen still supports is greater than the internal back-stresses which have developed in it. If negative creep -- i.e., strain recovery -- occurs, it is assumed that the back-stresses are greater than the remaining unit load. If specimen length remains constant it is assumed that the back-stress and unit load are equal.

By this method it has been determined that after 2% extension in tensile creep at 2500°C the average back-stress in ZTA graphite is about 2400 psi. After 10% extension it is about 2900 psi. If it is assumed that only that part of the applied load in excess of the back-stress is effective in producing further creep, then under these conditions about 1/4 of the applied load is still effective after 2% creep strain, and only about 1/10 is effective after 10% creep strain.

B. Mechanisms of Strain Recovery

When a large reduction in applied tensile load is made, negative creep -- in which the specimen actually shortens -- occurs in a strained graphite in spite of the fact that the specimen is still supporting the hanging weights which represent the reduced tensile load. The specimen does work in lifting these weights against gravity. The work done by the specimen has been computed to be about 10^6 ergs/cm^3 of specimen material in extreme cases among the strain-recovery tests so far made on ZTA graphite. This mechanical work obviously represents dissipation of energy which was somehow stored in the graphite during its previous strain history.

Two probable forms in which this energy might be stored in the graphite structure are as surface energy in new or enlarged cracks and voids, and as distortional energy associated with dislocations. For the case of cracks, the surface free energy is about 150 ergs/cm^2 when the cracks are parallel to the basal planes. For dislocations, the line-tension formula gives an energy of about 10^{-4} ergs/cm of dislocation line length when the averaging method of Hirth and Lothe is used for the elastic constant term, and about 10^{-6} ergs/cm when the shear modulus (C_{44}) for irradiation-hardened graphite is used.

To account for the work done by the specimen during recovery would require that about 10^4 cm^2 of crack surface be lost by a rehealing process per cubic centimeter of specimen. In the microstructure of ZTA graphite deformed in tensile creep, cracks about 0.01 cm in diameter are observed. If a rectangular grid of cracks of this size is assumed, a spacing between cracks of about 0.003 cm would be required to account for 10^4 cm^2 of surface per cm^3 of graphite. The number of cracks required would be reduced and their spacing increased if the surface area per crack were increased, for example by the webs which are frequently observed to span cracks in such materials as ZTA graphite. However, even without such an increment of surface area, the computed crack-spacing re-

quirement is realistic.

Alternatively, the length of dislocation that must be annihilated to satisfy this energy requirement is calculated to be about 10^{10} cm/cm^3 of graphite if the Hirth and Lothe value is used, and about 10^{12} cm/cm^3 if the C_{44} value for irradiated graphite is used. The value of 10^{12} cm/cm^3 is unrealistically large, but annihilation of 10^{10} cm of dislocation length per cm^3 of graphite appears possible.

At this point there is no basis for deciding which of these two possible forms of energy storage predominates in strained graphite, and it is probable that a significant amount of energy is stored in both forms. Surface-area measurements and transmission electron microscopy may provide information on which a decision can be made concerning the division of stored energy between them.

VII. THERMAL SHOCK

A. Equipment Calibration (P. E. Armstrong)

As a check on the method for measuring the power delivered by the electron beam in the CMF-13 thermal shock apparatus, a "Faraday cage" consisting of a water-cooled copper tube was installed. The beam could be directed into the tube and the collected current flow to ground measured. The temperature rise and flow rate of the cooling water could also be measured. Power calculated from beam current and voltage and from the water calorimeter are compared in Table XVI. The agreement indicated, to within 6%, seems adequate for this type of experiment.

TABLE XVI

ELECTRON BEAM POWER MEASUREMENTS

Beam Conditions			Calorimetric	
Current ma	Voltage kv	Power w	Measurements w	Difference %
190	9	1710	1694	0.9
245	9	2205	2089	5.3
300	9	2700	2657	1.6
355	9	3195	3002	6.0
400	9	3600	3418	5.1
440	9	3960	3739	5.6
475	9	4275	4029	5.8
485	9	4365	4121	5.6
500	9.2	4600	4345	5.5

B. The Effect of Specimen Diameter (P. E. Armstrong)

A series of thermal shock tests was made on 0.079-in. thick discs of POCO Grade AXF graphite in diameters from 0.500 in. to 1.125 in. Results are shown in Table XVII. Samples 1.000 and 1.125 in. dia which cracked did so only in the central region, indicating that failure occurred during cooling as a result of tensile stresses developed in a region which was plastically upset during heating. This does not represent thermal shock failure in quite the same sense as does cracking which occurs during heating and which originates outside of the directly heated central region of the specimens. If it is assumed that cracking confined to the plastically deformed region is not thermal shock failure, it appears that -- for AXF graphite in this thickness -- resistance to thermal shock produced by heating decreases rapidly with specimen diameter above about 0.625 in., and shows a minimum at a diameter of about 0.750 in.

Several other commercial graphites have been tested recently in thermal shock at this same specimen thickness but using only 0.500-in. dia discs. Some showed atypical behavior, and others could not be broken with the power available. The use of larger specimen diameters may make possible meaningful tests on these graphites with the existing thermal shock apparatus.

C. Figure of Merit for Thermal Shock (P. E. Armstrong)

The use of a figure of merit to predict relative thermal shock resistance of brittle materials is common, and has frequently been applied to graphites. Perhaps the most commonly used thermal shock index is $kS/\alpha E$ where k is thermal conductivity, S is ultimate tensile strength, α is thermal expansion coefficient, and E is Young's modulus. This index has been calculated as a function of temperature for CMF-13 Lot AAQ1 graphite (whose man-

TABLE XVII

THERMAL SHOCK TESTS ON 0.079-IN. THICK POCO AXF GRAPHITE [a]

Specimen Diameter, in.	Electron Beam Power, Watts								
	2585			3600			4500		
	Pass	Crack	Split	Pass	Crack	Split	Pass	Crack	Split
1.125	3	0	0				0	3[b]	2
1.000	4	0	0	3	0	3	0	1[b]	1
0.875							4	0	4
0.750				4	0	0	2	2	4
0.625							11	0	1
0.500							18	0	0

(a) Numbers in body of table indicate number of specimens which cracked, split, or did neither under each testing condition.

(b) Center cracks only.

TABLE XVIII

THERMAL SHOCK INDEX AS A FUNCTION OF TEMPERATURE, AAQ1 GRAPHITE

Temperature, °C	Thermal Conductivity, k, w/cm-°C	Tensile Strength, S, psi	Thermal Expansion Coefficient, α, $°C^{-1}$	Young's Modulus, E, 10^6 psi	Thermal Shock Index[a]
25	.310	3000	1.6	2.33	250
500	.191	3300	2.5	2.39	106
1000	.129	3400	3.6	2.54	48
1500	.103	3800	4.1	2.86	33
2000	.088	5000	4.4	3.15	32
2500	.084	6200	4.8	3.26	33

(a) Thermal Shock Index = $kS/\alpha E$. All properties are with-grain.

ufacture and properties were described in LA-3981). Results are listed in Table XVIII. The rapid decrease in calculated thermal shock index with increasing temperature does not agree with the behavior of AAQ1 or other graphites so far as this has been observed. The disagreement suggests that plastic deformation at the higher temperatures has a large influence on measured thermal shock resistance. Since plastic deformation is not expected below 1500°C, these calculations also suggest that in graphite a minimum in thermal shock resistance may exist between room temperature and 2000°C, perhaps in the vicinity of 1500°C.

D. Microscopy of Thermal Stress Damage (R. D. Reiswig, L. S. Levinson)

A large number of specimens tested in the CMF-13 electron-beam thermal-shock apparatus have been examined by optical and electron microscopy, in attempts to understand and characterize the structural damage produced by the test in a variety of graphites. Several rather general conclusions have been reached.

Cracks which form in graphite thermal-shock speci-

mens without actually fragmenting the specimen are in general of two types. In high-density graphites they tend to be tapered, with the wide end of the crack toward the center of the specimen. Such cracks are believed to have formed during cooling, as a result of irreversible upsetting of material near the center of the specimen which occurred during heating in the temperature region where graphite becomes plastic. Such cracks in graphites containing relatively large amounts of visible porosity tend not to be tapered. These are believed to have formed during heating, as a result of tension developed outside of the directly heated central region of the specimen, and to be unrelated to plastic deformation.

In cases where the binder residue is microscopically identifiable, it is observed that the path of the thermal-shock crack tends to detour filler particles except where the particle has a lamellar structure permitting easy cleavage and its lamellae are approximately parallel to the fracture path.

Specimens having relatively high thermal-shock resistance must, to produce failure, be heated for periods long enough so that a visible crater is usually produced, by vaporization of material at the point where the electron beam strikes the specimen. In general, when the binder residue can be identified, it is observed that in the region of the crater the binder residue has been vaporized preferentially. The filler particles which remain frequently show relatively smooth c-faces and quite rough a-faces, suggesting some vaporization from the ends of layer planes and very little from their surfaces. Particles of an isotropic filler, having random internal structures, appeared to have lost surface material nonselectively.

In pyrolytic graphites tested with the electron beam parallel to the average c-axis direction, delaminations are normally produced. In one specimen deformation twins were observed near the center of the area heated directly by the electron beam, where high radial compression might be expected to develop.

Microscopic examination sometimes reveals cracks not detected by visual inspection, and so indicates significant damage from thermal stresses in specimens which otherwise would have been considered unaffected by the test.

VIII. BORON-DOPED POLYCRYSTALLINE GRAPHITES

(P. Wagner)

A. General

Boronated graphites are available commercially, and do not represent a new area for research. The use of boric acid to "catalyze" graphitization was patented in 1894, and it was recognized in 1909 that -- with reference to the temperature coefficient of electrical resistance -- boron additions "chemically metallize" a graphite. Since about 1950 boronated pyrolytic graphites have been the subject of much solid-state research, and there is now a considerable body of knowledge concerning the effect of boron on the electrical and magnetic properties of pyrographite, particularly at low temperatures.

The CMF-13 work on boron-doped polycrystalline graphite was initiated to examine the relation between electrical and thermal conductivities in a system in which electrical conductivity could be controlled by a boron addition. As was reported in LA-4057-MS, this was accomplished but, because of an unexpected effect of boron on thermal conductivity, the further objective of elucidating conduction mechanisms in graphite was not achieved. In the meantime, the literature search which accompanied this work revealed many gaps and contradictions in published information on boronated graphites, and much speculation which seemed to be wrong more often than it was right. The CMF-13 series of boronated graphites was made under very close control and provided an unusual opportunity to examine an exceptionally uniform group of graphites in which the only significant variable was boron content. Characterization of these materials has produced a self-consistent set of data which can be used to correct many of the misconceptions that now exist concerning the effects of boron on polycrystalline graphite.

B. Graphite Preparation and Analysis

The extruded graphites made for this investigation were manufactured by J. M. Dickinson, CMF-13. The

green mix consisted of 67 parts Great Lakes Grade 1008-S graphite flour (CMF-13 Lot G-18), 12 parts Thermax carbon black (CMF-13 Lot TP-4), 21 parts furfuryl alcohol resin binder (Varcum 8251 plus 4% maleic anhydride catalyst), and a systematically varied proportion of fine metallic boron powder. Mixing, extrusion, and heat-treating procedures represented standard CMF-13 practice for resin-bonded graphites, and graphitization was in flowing helium at 2840 ± 40°C. So far as possible all members of the series were manufactured and heat-treated together, although comparison with boron-free but otherwise similar lots made at other times demonstrated that raw-materials variables and manufacturing processes were under good control. The uniformities of the graphites produced, including the uniformity of boron distribution in each graphite, were indicated by very low standard deviations of properties measurements. Electrical resistivity is particularly sensitive to variations in internal structure, and for an exceptionally uniform graphite (e.g., CMF-13 Lot AAQ1) the standard deviation of resistivity measurements may be as low as 2 to 3%. For all but two of the boronated graphites it was significantly lower than this.

Up to concentrations of 0.16% B, the boron added to the green mix appeared to remain fixed in the graphite structure throughout all manufacturing processes and all heat-treatments and temperature cycling (in both helium and vacuum) associated with properties measurements. Evidence for this was: (a) Spectrochemical analyses of the as-graphitized and of the tested samples, made by LASL Group CMB-1, agreed well with each other and with the proportion of boron added to the green mix. (b) None of the measured properties changed detectably with prolonged or repeated high-temperature heat treatment. (This of course also attests to the stability of the graphite structure.)

At higher boron concentrations it appears that boron may have been lost from the graphite during long heat-treatments. This was not firmly established because in this composition range boron concentrations are too high for accurate spectrochemical analysis and too low for precise gravimetric analysis. However, electrical resistivity was observed to change with continued heating, in a direction suggesting progressive reduction in boron content.

X-ray diffraction measurements by J. A. O'Rourke, CMF-13, showed a systematic decrease in interplanar spacing of the graphite, d_{002}, with increasing boron concentration. This is illustrated by Fig. 9. (On the basis of less-precise, preliminary measurements, it was reported in LA-4057-MS that d_{002} did not change with boron concentration. This was incorrect.) No evidence was found for the presence of a second phase-- boron carbide -- up to the maximum concentration considered, 0.79% B. Apparent crystallite size, L_c, was essentially the same at all boron concentrations, and was in the range 420 to 450 Å, representing well-graphitized material. Crystalline anisotropies, as represented by the Bacon anisotropy factor, were essentially the same for a sample containing 0.79% B (σ_{ox}/σ_{oz} = 1.503) and for an undoped control sample (σ_{ox}/σ_{oz} = 1.514), so that it is unlikely that degree of preferred orientation varied significantly throughout the series.

In uniformity and consistency, this group of boronated polycrystalline graphites is believed to be superior to any on which investigations previously reported in the literature have been performed.

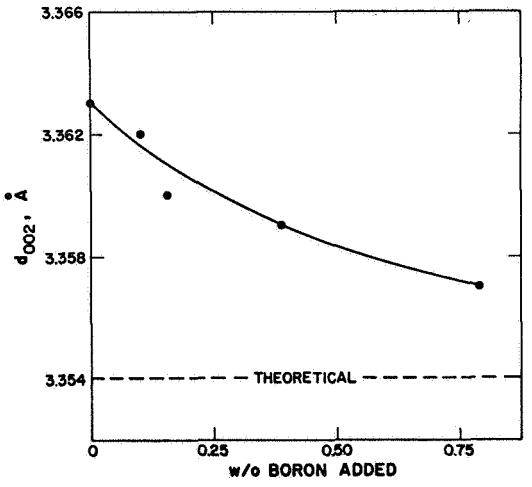

Fig. 9. The effect of boron on the interplanar spacing (d_{002}) of a polycrystalline graphite.

C. Properties

The effect of boron additions on the electrical resistivity of graphite is detailed in the literature, but in a rather curious manner. Weintraub in 1909 recognized that the addition of boron changed the temperature coefficient of resistivity of graphite from a negative to a positive value. This information was ultimately utilized by the Bell Laboratories in 1950 to produce pyrographite film resistors with just enough boron added to keep the resistivity constant with temperature. Despite the obvious conclusions to be drawn from these experiments, the most commonly encountered statement in the literature on boronated graphites is that -- in the concentration range covered by the present work -- the addition of boron decreases electrical resistivity. This statement is of course based on room-temperature data, such as that plotted in Fig. 10. That this correlation of resistivity with boron content is fortuitous is demonstrated by Fig. 11, where resistivity is plotted as a function of temperature for graphites of various boron contents. At any temperature significantly above room temperature the correlation breaks down. This set of curves does, however, give a relatively complete and self-consistent picture of the effects of both boron and temperature on the electrical resistivity of a polycrystalline graphite. The composition 0.081 % B is particularly interesting, since the graphite having this boron content has electrical resistivity which is constant within a 5% band over a temperature range of 2500°C.

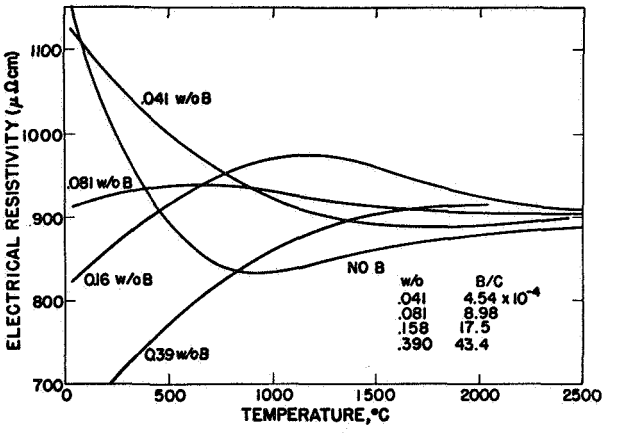

Fig. 11. The effect of temperature on the electrical resistivity of boron-doped polycrystalline graphites.

Fig. 12 shows the effect of boron concentration on dynamic Young's modulus measured at room temperature. As might be expected from the decreasing interplanar spacing shown in Fig. 9, increasing boron content significantly increases Young's modulus of polycrystalline graphite.

The effect of boronation on room-temperature thermal conductivity (Fig. 13) is somewhat surprising, since it has been both theorized and reported that boron additions up to about 0.1% have no effect on thermal conductivity. The decrease in thermal conductivity shown by the curve

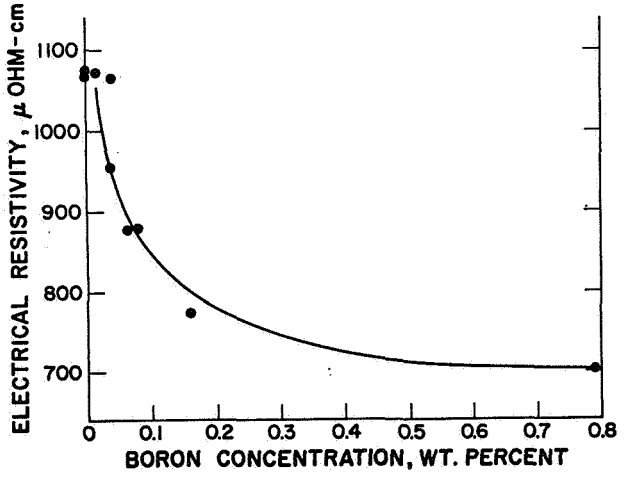

Fig. 10. The effect of boron on the electrical resistivity of polycrystalline graphite at 23°C.

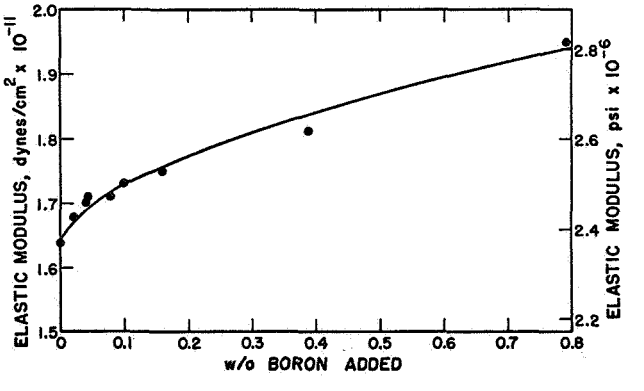

Fig. 12. The effect of boron on the dynamic Young's modulus of polycrystalline graphite at 23°C.

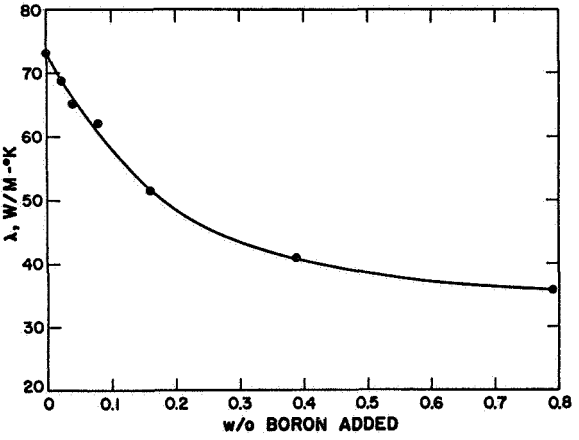

Fig. 13. The effect of boron on the thermal conductivity of polycrystalline graphite at 23°C.

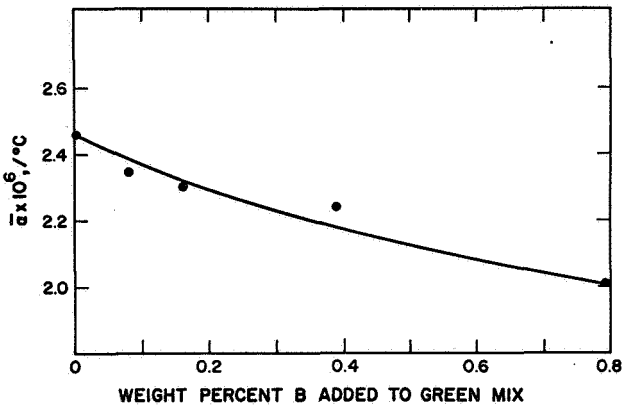

Fig. 15. The effect of boron on the average thermal expansion coefficient of polycrystalline graphite between room temperature and 645°C.

between zero and 0.1% boron is about 20%, and the uncertainty of the flash-diffusivity method used to measure conductivity is probably not greater than 7% in the worst case. The decrease shown is therefore believed to be real.

In Fig. 14 thermal conductivity is plotted as a function of temperature for a series of boron-doped graphites. In this case the correlation between thermal conductivity and boron content is maintained over the interval -100°C to about 1000°C. However, the differences are modified as temperature increases. The vertical bar drawn at 1700°C shows the effect on the conductivity value of an experimental error of 1°C in the measurement of ΔT at that temperature. In view of this uncertainty, which increases toward the lower limit of usefulness of the technique used above 1000°C, it is not clear that the curves actually cross as indicated at about 1100°C and about 2000°C, or that there is any real difference among them above about 1500°C. However, in the lower temperature region the uncertainties are less, and the confidence level is high that the maximum values shown are in the proper sequence.

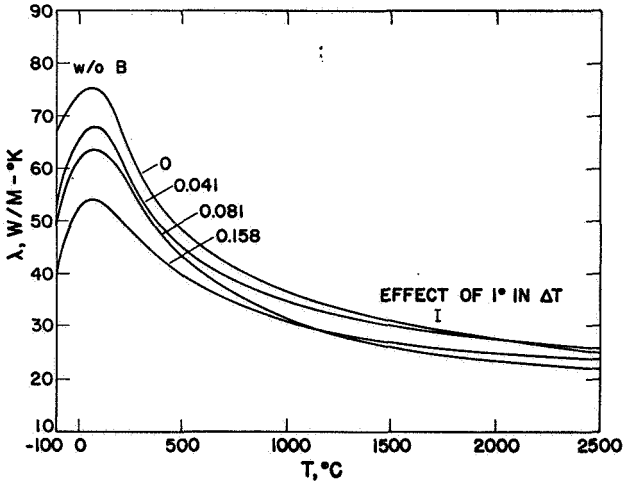

Fig. 14. The effect of temperature on the thermal conductivity of boron-doped polycrystalline graphites.

Measurements were also made of the thermal expansion behavior of the boron-doped graphites. In Fig. 15 the average coefficient of thermal expansion over the temperature interval 23-645°C is plotted as a function of boron content. It is the c-direction expansion of the single crystal which is the major contributor to thermal expansion of a polycrystalline graphite, and reduced interplanar spacing -- implying stronger interlayer bonding -- might be expected to reduce c-direction expansion. Because of the effect of boron on interplanar spacing, shown in Fig. 9, it is not unexpected that the thermal expansion coefficient decreases with increasing boron content.

D. Discussion and Conclusions

From the data collected on this series of graphites it is clear that some of the generalizations concerning boronated graphites which have appeared in the literature must be revised or carefully modified.

It is frequently stated that small boron additions enhance graphitization. Unless degree of graphitization is measured solely by interplanar spacing, this is evidently incorrect. Graphitization is usually considered to involve an increase in crystallite size and to be accompanied by an increase in thermal conductivity and decreases in elastic modulus and electrical resistivity. The addition of boron does reduce d_{002}, but with no measurable effect on L_c. It increases elastic modulus and reduces thermal conductivity. Its effect on electrical resistivity is complex. Obviously, any statement concerning the effect of boron on graphitizing processes must be very carefully qualified.

In general the effect of boron on electrical resistivity and the effect of temperature on the resistivity of boron-doped graphites have been discussed independently of each other. It is apparent from Fig. 11 that this is misleading and can be very confusing. The effect of boron on resistivity varies with temperature, and the effect of temperature varies with boron content. The two variables must be considered together.

The positions occupied by boron atoms in the graphite structure are still not known. In the concentration range here considered no microscopic or x-ray evidence has been found for existence of a second phase, and d_{002} decreases as boron content increases over the entire interval. Apparently, up to at least 0.79 wt % B, the boron atoms do enter the carbon structure, which by definition represents solid solubility. At and below 0.16 wt % B they are firmly bound in the structure, and at higher concentrations perhaps less firmly bound. Qualitatively this is consistent with statements in the literature that the "solubility" of boron or its "substitutional limit" is "a few tenths of one percent". The effects of boron on interplanar spacing and on thermal conductivity are difficult to explain except by substitution of boron atoms for carbon atoms within the layer planes of the graphite structure. However, neither property curve changes slope discontinuously at any boron concentration in the range considered, so that neither gives direct evidence of a substitutional solubility limit. The possibility remains that at least part of the boron atoms are concentrated at crystallite boundaries or other discontinuities in the graphite structure. An appreciable interstitial solubility, with boron atoms between the layer planes, seems very unlikely.

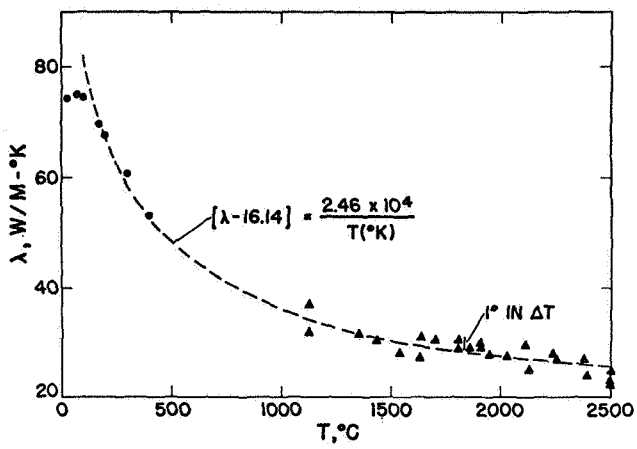

Fig. 16. Thermal conductivity of a polycrystalline graphite as a function of temperature, showing a 1/T temperature-dependence.

Early in this investigation it was hoped that the relation $\lambda = \lambda_e + \lambda_L$ might be used to separate the electronic (λ_e) and lattice (λ_L) components of thermal conductivity. λ_e was to be computed from electrical resistivity, absolute temperature, and the Lorenz number. However, it is clear from the wild variations of resistivity with boron content and temperature shown in Fig. 11 and the regular variation of λ shown in Fig. 14 that a constant Lorenz number cannot be assumed. This part of the investigation was therefore not successful. However, something can be deduced about conduction mechanisms from the temperature-dependence of λ.

In recent years there has been speculation in the literature that at temperatures above 1800 or 1900°C thermal conduction in graphite is entirely electronic in nature rather than largely by lattice conduction, which is the classical view. For purely electronic conduction λ will vary directly with the electron-phonon interaction, which has a small temperature dependence. For lattice wave conduction λ will be limited by Umklapp processes, which vary as 1/T. Figure 16 shows the λ vs temperature data for the unboronated graphite of this series, with a 1/T curve superimposed on it. The fit is good over a 2300°C temperature interval. From the similarity of the curves in Fig. 14 it

is evident that a 1/T curve can also be fit to all of the data collected on boron-doped graphites, and this is true of data previously collected on a wide variety of other graphites. It appears that up to at least 2500°C the electronic component of thermal conduction must be completely overshadowed by the lattice contribution.

IX. "WHITE" CARBON

(P. E. Armstrong, J. M. Dickinson, J. A. O'Rourke, R. D. Reiswig, L. S. Levinson)

It was reported at the Ninth Carbon Conference, and more recently in Science (165, 589), that a "white" allotropic form of carbon had been produced at high temperatures and low pressures during sublimation experiments on graphite. This is said actually to be a transparent material formed as a thin coating on the graphite, consisting of very fine crystals and appearing white because of light scattering from the many crystal surfaces. Its structure is stated to be hexagonal with unit cell dimensions $a_o = 8.945$, $c_o = 14.071$, and it is apparently the same substance recently discovered in a graphitic gneiss from the Ries Crater in Bavaria (Science 161, 363).

Several attempts have been made by CMF-13 to produce and identify "white" carbon, so far with no success. White or grayish-white deposits have been examined from the surfaces of: graphite grips from a high-temperature creep furnace; the craters eroded into the heated surfaces of a variety of graphite and pyrographite thermal-shock specimens; pyrographite cylinders electron-beam heated and insulated (with graphite foil) in various ways to produce a variety of temperature gradients; a similarly heated pyrographite cylinder whose surfaces had been impregnated with fine silicon carbide; other pyrographite cylinders containing drilled holes, with the electron beam focussed either near the top or near the bottom of the hole; and a rectangular pyrolytic graphite bar heated to burnout by electrical current flow through it. The deposit on the graphite grips was identified as hydrated calcium oxide. In all other cases only normal pyrolytic graphite could be detected, and the white appearance was the result of reflections from many small, relatively smooth, pyrographite surfaces.

It is evident that the "white" allotrope of carbon is difficult to produce, or to isolate, or to identify, and perhaps difficult in all of these respects.

X. FUEL-ELEMENT CRACKING

(R. D. Reiswig, L. S. Levinson)

An experimental graphite fuel element containing pyrocarbon-coated fuel particles has been examined by optical and electron microscopy in an attempt to discover the cause of microcracks known to exist in the graphite matrix. The element was extruded from a mix containing a reground POCO graphite filler, Thermax carbon black, and a Varcum furfuryl alcohol resin binder, and was graphitized at a relatively low temperature.

Typically the microcracks ranged in length from 50 to 200 μ and were roughly lenticular in section, suggesting that the matrix was plastic when they were formed. They were randomly oriented in both transverse and longitudinal sections of the element, in no apparent relation to the flow of material during extrusion, so that they are believed not to have been produced by the extrusion process. On the walls of many of the microcracks there were stringy projections of binder residue containing particles of carbon black, and occasionally these bridged the crack completely. This is believed to indicate that the crack was formed while the resin was in a slightly tacky condition. In other cracks the walls were free of such projections, and it appeared that opposite surfaces would match well if the crack were collapsed and its sides brought together. These were probably formed while the matrix was still somewhat plastic but after the binder had passed the tacky stage.

It is believed that these microcracks were formed by the evolution and expansion of gases during the curing heat-treatment, at a rate greater than that at which they could escape to a free surface. They were probably formed over a range of relatively low temperatures including temperatures at which the binder was tacky and also higher temperatures at which it was not tacky but was still plastic. The indication of plastic accomodation of the

matrix to cracks opening within it implies that these cracks were formed before the matrix became rigid, and therefore in advance of the baking and graphitizing heat treatments. Their incidence can probably be reduced by reducing the heating rate during curing.

Fine cracks typical of graphite structures in general, and probably formed during baking or graphitizing, were also observed, in concentrations normal for a graphite made from a filler having a high coefficient of thermal expansion. Some of these were at interfaces between filler and binder, but more were within the binder. Not infrequently they connected fuel particles, usually meeting the particle along a radial direction. Occasionally the crack turned to follow the surface of the fuel particle's pyrocarbon coating, but in no case was the crack observed to penetrate the pyrocarbon coating.

The distributions of filler, carbon black, and binder were quite uniform, and wetting of filler and fuel-particle surfaces by the binder appeared to be thorough, indicating good mixing and conditioning of the raw mix. There was some tendency of fuel particles to appear in groups or short chains, although this was not pronounced. In the reground POCO graphite filler there appeared to be a deficiency of particles in the 20-30 μ range, which probably contributed to the occasional presence of small porous regions in the microstructure. The larger filler particles (over about 50 μ dia) contained pore distributions typical of the POCO graphites, which were not accessible to the binder used in fuel-element manufacture.

This is a well-made graphite. Its principal deficiency, the relative large, lenticular microcracks, probably resulted in large part from the good packing characteristics of the filler, which made gas escape difficult. These cracks can probably be minimized by curing the element very slowly. Its other deficiencies are typical of a high-quality graphite made from a high-expansion filler, but could probably be reduced by improving the particle-size distribution of the filler. Since mixing was apparently very good, there is no obvious way to improve the distribution of fuel particles.

XI. DENSITY SEPARATION OF GRAPHITE COMPONENTS

(R. D. Reiswig)

In an investigation of the graphitization of furfuryl alcohol resin binders, described above, a vitreous-carbon filler was used. After the graphitizing heat-treatment the filler and binder residue were separated by crushing the specimen and sieving the crushed product. The fine fraction produced consisted principally of binder residue, but did still contain about 10 to 30% of vitreous-carbon filler material. This appeared to be due primarily to comminution of filler particles during crushing of the sample rather than to incomplete freeing of one component from the other. In view of the low particle-density of vitreous carbon, it therefore seemed possible that a better separation might be achieved by a sink-float separation in a high-density medium.

Accordingly, a solution of tetrabromoethane and carbon tetrachloride was prepared at a density of 1.97 g/cm^3. The fractions previously separated by screening were recombined and ground lightly with a pestle and mortar, and the sink-float separation was attempted. Microscopic examination of the more dense fraction, which sank in the heavy liquid, showed that it contained not more than about 1 to 2% of vitreous-carbon filler material.

In this case the sink-float separation is considered to have been very successful. It is not clear that it can be applied as well to systems in which fillers other than vitreous carbon have been used. However, it has the advantage that the filler particles or other components separated need not be carefully sized, and the technique is relatively quick and simple. It is expected to be useful in other investigations.

XII. PORE PRESERVATION IN METALLOGRAPHY

(R. D. Reiswig)

During microscopic examination of thermally shocked specimens of AAQ1 graphite, it became important to decide to what extent the void structure observed was produced by the thermal shock test. Many of the shocked

specimens mounted in epoxy resin for microscopic examination appeared to have significantly more epoxy-filled voids than had been observed previously in untested material. However, it was recalled that epoxy-filled porosity of about the same type and degree had previously been noted in about the first 0.015 in. below the surface of epoxy-mounted specimens of the untested graphite. Grinding and polishing to greater depth had produced a nearly featureless surface, and it was supposed that voids near the surface had been produced mechanically during cutting of the section. The dense-appearing material further from the surface was assumed to represent the true structure of the graphite. If this was correct, then in AAQ1 graphite the thermal-shock test had created widespread porosity.

To examine this effect further, a section of AAQ1 graphite prepared by normal methods was impregnated at high pressure with the epoxy resin usually used to mount specimens. This was done at room temperature in a standard metallographic mounting die under pressure of 4000 to 5000 psi, which was maintained for 15 min. The pressure was then relieved and the specimen removed and cured as usual at 15 psig. In this case, instead of occupying only the top 0.015 in. of the section, the same type and degree of porosity were found to extend to more than 0.050 in. below the initial free surface. Because the pressure was applied hydrostatically, it is felt that the only structural damage produced by it was a breakdown of separations between previously unconnected voids. The epoxy-filled void structure near the specimen surface may, then, be misleading with regard to degree of interconnectedness of the original pore structure, but otherwise it is probably representative of the size, shape, and distribution of voids initially present in the graphite. If so, the thermal shock test had no significant effect on the void structure of AAQ1 graphite.

CMF-13 has probably been misled in this way in the past concerning the pore structures of other dense graphites which, at ordinary pressures, are poorly penetrated by the mounting resin. It is not obvious how pores which are not filled with mounting resin can disappear from the specimen surface. Presumably they become packed with polishing debris, and perhaps this is covered over by flow of adjacent surface material. In any case, it is evident that great care is necessary in examining the void structures of high-density graphites, and a search is continuing for an epoxy-hardener system which may penetrate such graphites to greater depth under normal pressures.

XIII. POCO GRAPHITES

(P. Wagner)

A. Thermal Expansion Measurements

The coefficients of thermal expansion of the group of POCO graphites described in LA-4057-MS and LA-4128-MS have been determined and are listed in Table XIX. The values given are averages over the temperature range 23°C to 645°C. The specimens tested were machined from round bars purchased from Poco Graphite, Inc. In each case it was assumed that the cylinder axis of the bar was the with-grain direction and a direction normal to this was an across-grain direction. As can be seen from the table, all grades tested had very high thermal-expansion coefficients and were nearly isotropic in this regard, as they were in the other properties listed in LA-4057-MS.

B. Grade AXM-5Q1 Graphite

POCO Grade AXM-5Q1 is the intermediate-density POCO graphite, in this case graphitized at 2500°C and halogen-purified. Its thermal expansion over the temperature range ambient to 2000°C was discussed in LA-4171-MS.

The three-dimensional anisotropy of a 7.5 in. by 4 in. by 5 in. plate of AXM-5Q1 graphite was investigated by room-temperature property measurements made on specimens machined in three orthogonal orientations parallel to the edges of the plate. Bulk density of the graphite was 1.764 to 1.768 g/cm^3, and x-ray diffraction measurements gave a Bacon anisotropy factor of 1.00 to 1.01. Electrical resistivities, thermal expansion coefficients, and thermal conductivities in the three directions are listed in Table XX, where the X direction is parallel to the 7.5-in. dimension of the plate, Y is parallel to the 5-in.

TABLE XIX

THERMAL EXPANSION COEFFICIENTS

OF POCO GRAPHITES

POCO Grade	Thermal Expansion Coefficient[a] With-Grain	Across-Grain
AXZ	7.67	7.64
AXZ-QB	7.01	7.00
AXZ-QBG	7.19	7.95
AXZ-9Q	7.42	7.58
AXF	8.39	8.38
AXF-QB	7.80	7.89
AXF-QBG	8.10	8.33
AXF-9Q	7.15	8.15

(a) Average, 23°C to 645°C

TABLE XX

ROOM-TEMPERATURE PROPERTIES

OF AXM-5Q1 GRAPHITE

Direction:	X	Y	Z
Electrical Resistivity, μΩcm	1630	1650	1620
CTE, $x10^{-6}/°C$[a]	7.62	7.89	7.75
Thermal Conductivity, W/M-°K	75	77	79

(a) Thermal expansion coefficient, average, 23°C to 645°C

dimension, and Z is parallel to the 4-in. dimension.

These measurements indicate that this plate of POCO AXM-5Q1 graphite was almost perfectly isotropic.

XIV. PUBLICATIONS RELATING TO CARBONS AND GRAPHITES

Smith, M. C., "CMF-13 Research on Carbon and Graphite, Report No. 9, Summary of Progress from February 1 to April 30, 1969", LASL Report No. LA-4171-MS, May, 1969.

Lewis, H. D., "The Problem of Characterization of Graphite Powders", Published Lecture Notes, UCLA Engineering and Physical Sciences Extension Short Course Engr. 847.23, February, 1969.

Lewis, H. D., "Small Particle Statistics: The Analysis of Particle 'Size' Data", Published Lecture Notes, UCLA Engineering and Physical Sciences Extension Short Course Engr. 847.23, February, 1969.

Wagner, P., and Dauelsberg, L. B., "Some Thermal Properties of a Polyfurfuryl Alcohol Bonded Graphite", Carbon 7, 273 (1969).

Smith, M. C., "A Reply to the Comments of Wade and Gillis", Carbon 7, 333 (1969).

Weertman, J., "Effect of Cracks on Creep Rate", ASM Transactions Quarterly, Vol. 62, pp. 502-511, (1969).

Green, W. V., Zukas, E. G., and Weertman, J., "Effect of Cracks on Creep Rate - Part II (Experimental)", ASM Transactions Quarterly, Vol. 62, pp. 512-520, (1969).